1968

The effect of gamma radiation on the conductivity of sodium chloride

Michael Claudewell Jon Carlson
Iowa State University

69-4221

CARLSON, Michael Claudewell Jon, 1939-

THE EFFECT OF GAMMA RADIATION ON THE CONDUCTIVITY OF SODIUM CHLORIDE.

Iowa State University, Ph.D., 1968
Engineering, nuclear

University Microfilms, Inc., Ann Arbor, Michigan

THE EFFECT OF GAMMA RADIATION ON THE CONDUCTIVITY OF SODIUM CHLORIDE

by

Michael Claudewell Jon Carlson

A Dissertation Submitted to the
Graduate Faculty in Partial Fulfillment of
The Requirements for the Degree of
DOCTOR OF PHILOSOPHY

Major Subject: Nuclear Engineering

Approved:

Signature was redacted for privacy.

In Charge of Major Work

Signature was redacted for privacy.

Head of Major Department

Signature was redacted for privacy.

Dean of Graduate College

Iowa State University
Of Science and Technology
Ames, Iowa

1968

TABLE OF CONTENTS

INTRODUCTION

The developement of electrical insulating materials suitable for use in high temperature, high radiation intensity fields is of considerable interest for direct energy conversion devices, nuclear rockets and other areas in which electrical leads are used under conditions of high temperature and high radiation field intensity. As a result, there is need for research directed toward understanding the mechanism by which radiation alters the conductivity of electrical insulators.

Expressions for the electrical conductivity of a number of insulating materials have been developed (1, 2) on the assumption that the total conductivity can be expressed as the sum of the conductivity of the unirradiated material and a radiation intensity dependent term. This assumption implies that the conduction mechanism acting in the unirradiated material remains unaltered by the radiation or at least that the change can be taken into account by the radiation induced conductivity term.

While this approach has been successful in some materials, especially in insulating materials in which the major portion of the conduction is by electronic carriers, the conductivity of some other materials is known to decrease, such as for those materials in which ion diffusion is a significant charge conduction mechanism. In this case, treatment of the total conduction as due to a diffusion carrier term plus a radiation induced conduction term still has considerable merit, but the diffusion carrier term can no longer be chosen simply as the conduction term of the unirradiated material. Many alkali halide materials are

of this latter type.

Since considerable evidence indicates that conduction in the alkali halides is proportional to the vacancy concentration, and one of the primary effects of irradiation on the structure of many ionically bonded materials is vacancy introduction, it appears that the alkali halide materials should be useful in examining the effect of irradiation on this type of material.

As a result, an investigation was undertaken to determine the effect of Co^{60} gamma radiation on the conduction behavior of single crystalline NaCl.

CONDUCTIVITY OF UNIRRADIATED NACL

Total Conductivity

The total conductivity, σ_T, of a single crystal of sodium chloride can be given by the expression

$$\sigma_T = \sum_{i=1}^{n} \sigma_i \qquad (1)$$

where the individual conductivity terms, σ_i would include terms for conduction by defects, electronic conduction, impurity atom conduction etc., if it is assumed the carrier concentrations are independent of one another. This behavior can also be expressed as

$$\sigma_T = \sum_{i=1}^{n} n_i q_i \mu_i \qquad (2)$$

where n_i is the concentration of the ith carrier, q_i is the charge on the ith carrier and μ_i is the mobility of the ith carrier.

Comparison (3) of the available diffusivity and conductivity data for sodium chloride has led to the conclusion that the steady state d.c. conductivity of the crystal was due predominantly to positive ion vacancies, since the total observed conductivity of the crystal was essentially equal to the conductivity calculated from diffusivity data for the sodium ion in NaCl using the Nernst-Einstein equation. More recent work (4) has led to the conclusion that the contribution of the chlorine ion can be considerable under some conditions and cannot always be ignored, especially if the specimen is polycrystalline.

Cation Conduction

A typical plot of conductivity versus reciprocal temperature for NaCl is shown in Figure 1 for the temperature region of interest in this experiment (5).

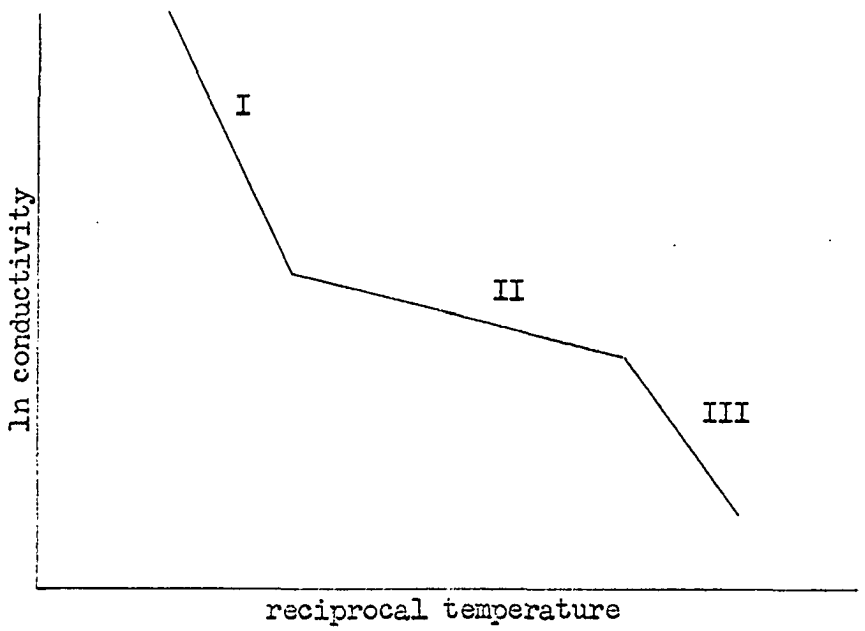

Figure 1. Logarithm of conductivity versus reciprocal temperature

Cation conduction in the intrinsic region (region I of Figure 1) is usually assumed to be due to ionic conduction under the condition that the concentration of Schottky pairs (the predominant defect appearing in NaCl single crystals in this temperature range) is set by thermal equilibrium (3, 6). Cation vacancy conduction can be given by the expression

$$\sigma = n q \mu \qquad (3)$$

in which μ, the mobility of the cation vacancy, is given by the expression

$$\mu = \frac{4\, e\, a^2\, \nu_o\, e^{\Delta S_m/k}\, e^{-\Delta E_m/kT}}{kT} \qquad (4)$$

where e is the unit electronic charge, a is the lattice parameter, ν_o is the effective lattice vibration frequency, k is Boltzmann's constant, T is the absolute temperature, ΔS_m is the entropy increase associated with vacancy motion and ΔE_m is the activation energy associated with vacancy motion. q = e since the cation is singly charged and n, the cation vacancy concentration is given by the expression

$$n = N\, e^{(\Delta S_f/2k - \Delta E_f/2kT)} \qquad (5)$$

where $\Delta S_f/2$ is one half the entropy increase associated with the formation of a Schottky pair and $\Delta E_f/2$ is one half the activation energy associated with the formation of a Schottky pair. Then

$$\sigma = \frac{4\, e^2\, a^2\, \nu_o\, e^{-(\Delta S_m/k + \Delta S_f/2k)}\, e^{-(\Delta E_f/2kT + \Delta E_m/kT)}}{kT} \qquad (6)$$

which can be written as

$$\sigma = \frac{\sigma i_o}{T}\, e^{-\left[\frac{\Delta E_f + 2\Delta E_m}{2kT}\right]} \qquad (7)$$

As can be seen from this expression, the activation energy for the intrinsic region, $E_{intrinsic}$, is given by the expression

$$\Delta E_{intrinsic} = \frac{\Delta E_f + 2\Delta E_m}{2} = \frac{k \ln \frac{\sigma_1}{\sigma_2} + k \ln \frac{T_1}{T_2}}{\frac{1}{T_2} - \frac{1}{T_1}} \qquad (8)$$

where σ_1 and σ_2 represent the conductivities at two temperatures, T_1 and T_2 respectively, within the intrinsic region. In region II of Figure 1, the extrinsic region, the carrier concentration is usually assumed to be a constant, with the result that the conductivity is given by the expression

$$\sigma = \frac{4 e^2 a^2 \nu_o e^{-\Delta S_m/k}}{kT} e^{-\Delta E_m/kT} = \frac{\sigma e_o}{T} e^{-\Delta E_m/kT} \qquad (9)$$

The expression for the activation energy in this region is then given by

$$\Delta E_m = \frac{k \ln \frac{\sigma_3}{\sigma_4} + k \ln \frac{T_3}{T_4}}{\frac{1}{T_4} - \frac{1}{T_3}} \qquad (10)$$

where σ_3 and σ_4 represent the conductivities at two temperatures, T_3 and T_4 respectively, within the extrinsic region. In region III, the association region (7, 8), the cation vacancy is assumed to be bound by its virtual negative charge to polyvalent impurity atoms. As a result, the slope in this region is usually set equal to $(\Delta E_m + \Delta E_i)/k$ where E_i is the binding energy of the vacancy to the polyvalent impurity.

Anion Conduction

While the conduction by ionic crystals is usually presumed to be due to the cation vacancy, anion vacancies are also expected to be present in ionic crystals (6). A recent examination (9) of the behavior of the equilibrium anion vacancy concentrations is based on the idea that a space charge builds up next to free surfaces, dislocations and other defect sources and sinks. Using this assumption, the conclusion is reached that in intrinsic ionic materials the electrical neutrality of the crystal is maintained by the presence of an equilibrium space charge potential, ϕ_∞, which leads to an increase in the energy required to produce a cation vacancy, E_m^+, and a decrease in the energy required to produce an anion vacancy, E_m^-, so that

$$E_m^+{}_{\text{effective}} = E_m^+ + e\phi_\infty = E_m^-{}_{\text{effective}} = E_m^- - e\phi_\infty. \qquad (11)$$

In this expression it is assumed that $E_m^+ < E_m^-$. If $E_m^- < E_m^+$ the sign of the space charge terms would be reversed so that $E_m^+{}_{\text{effective}} = E_m^-{}_{\text{effective}}$ would be maintained. Further examination leads to the conclusion that divalent positive ions decrease the equilibrium anion vacancy concentration, introducing a reciprocal relationship between the cation and anion vacancy concentrations. Experimental results which can be interpreted in a manner compatible with the results of space charge theory studies have been obtained in anion diffusion studies utilizing tracer techniques (10, 11, 12). In these studies the diffusion coefficient for anion vacancies is shown to decrease significantly with small additions of divalent calcium ion, however, it is found that

with larger additions the depression of the diffusion coefficient saturated. The observed change in the activation energy associated with the anion diffusion process as the concentration of divalent impurities was increased was interpreted as a change in the diffusion mechanism of the anion tracer from the diffusion of single anion vacancies to anion movement by neutral vacancy pair diffusion. This is compatible with the results of the space charge study, if it is assumed that the space charge induced reciprocal relationship between equilibrium positive and negative ion vacancy concentrations is brought about by neutral vacancy pair formation, and that the neutral vacancy pairs formed are free to diffuse.

Since on the basis of diffusion studies anion vacancies can be assumed to be present and capable of motion, they should conduct current in a crystal when a voltage is applied. However, since it is not necessary to subtract an anion contribution from the total conductivity found using d.c. applied voltages in order to get agreement between the results of steady state d.c. conductivity measurements and sodium ion diffusion measurements (12, 13) it appears that the steady state motion of halide ions is blocked by some means. Measurements using a.c. applied voltages, however, do give a total conductivity which can be interpreted as the sum of two ionic contributions (4, 14). Since the two contributions to the a.c. ionic conductivity show the same particle size dependence reported for sodium ion and chloride ion diffusion, it seems likely that the additional carrier found with a.c. measurements is the chloride ion vacancy. When the additional ionic conductivity found in a.c. measurements is plotted versus reciprocal temperature, the acti-

vation energy calculated from the slope is found to be the same as the activation energy predicted for the motion of the chloride ion vacancy by chloride ion diffusion studies in "pure" sodium chloride over the temperature range covered in this experiment (4).

Time-Dependent Conductivity

Polarization behavior, which leads to time dependence of the conductivity for many materials has been known for some time. The existence of electronic, ionic and dipole orientation contributions to the total polarization has been observed in many ionic materials (6), including sodium chloride. Several different dipole orientation mechanisms, each with a characteristic time constant have been observed for sodium chloride (7, 15, 16).

An additional polarization mechanism which has a time constant on the order of minutes has been observed in sodium chloride. Since a time constant of this duration would seem to be much longer than a simple dipole rotation requires, and in view of the fact that the current due to the chloride ion vacancy appears to be blocked, this polarization mechanism has been identified as due to the blocked current of the chloride ion vacancy (4).

A plot of current flowing in a crystal as a function of time, t, after a constant voltage has been applied is shown in region I of Figure 2. Region II shows the behavior of the current when the polarity of the applied field is reversed.

The current flowing in the dielectric material, $I_{(t)}$, when a field of magnitude E is applied suddenly is proportional to the first derivative

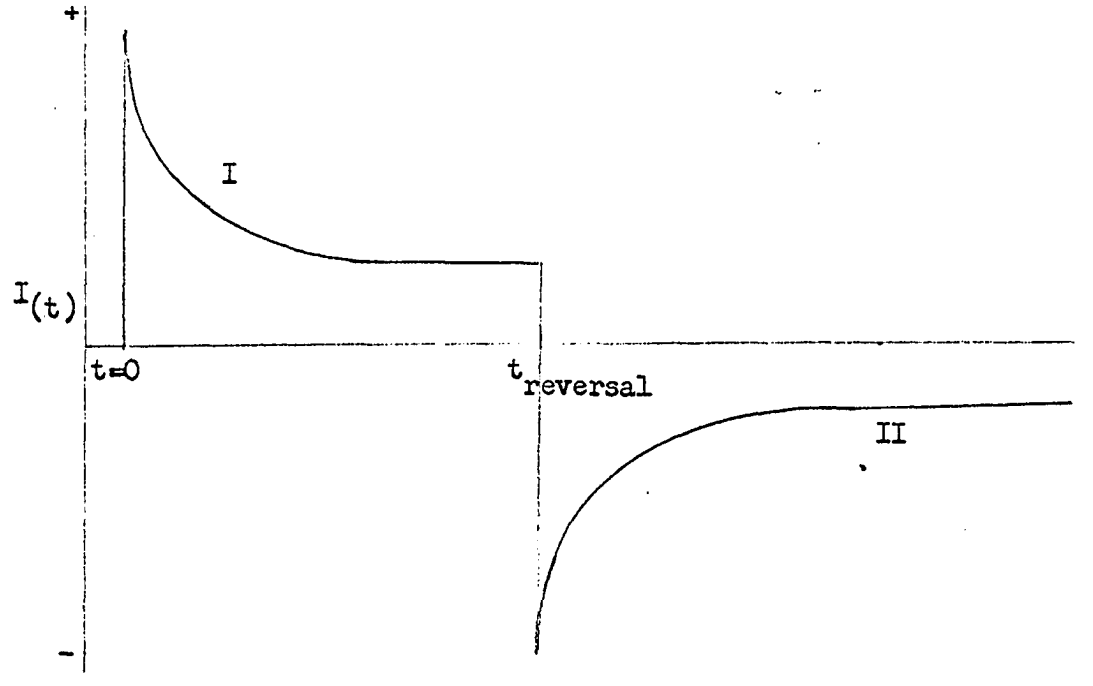

Figure 2. Time dependent current

of the displacement, D, where an expression for the displacement can be written (6)

$$D_{(t)} = \epsilon_s E - \left[-D_{(o)} + \epsilon_s E\right] e^{-t/\tau} \qquad (12)$$

Then

$$I_{(t)} \propto \frac{dD_{(t)}}{dt} \propto 0 + \frac{\epsilon_s E}{\tau} e^{-t/\tau}$$

or

$$I_{(t)} \propto e^{-t/\tau}$$

where ϵ_s is the static dielectric constant, E is the applied field, $D_{(o)}$ is the initial value of D, t is the time and τ is the time constant

for the relaxation process. From this it can be seen that a plot of ln $I_{(t)}$ versus time will give a straight line plot whose slope is $-1/\tau$. If more than one relaxation process (polarization process) is present, standard analytical techniques can be applied. In this case, since it was desired to study the effect of the radiation on the ionic conductivity, only one extrapolation was necessary to yield the initial long time constant polarization current which was assumed to be proportional to the chloride ion vacancy as discussed above.

IRRADIATION INDUCED DEFECTS IN NACL

Defect Production Mechanisms

Defects in sodium chloride single crystals can be created thermally or by any of several extrinsic mechanisms, including irradiation of the crystal at temperatures too low for complete annealing to occur.

Since the type and concentration of each defect which is found in a crystal after irradiation depends strongly upon the irradiation temperature it is desirable to consider irradiations which have been carried out at liquid helium temperatures because defect interactions are very slow at this temperature. Early work on the formation of absorption centers in ionic crystals by irradiation at liquid helium temperature was carried out on alkali halides by Duerig and Markham (17). It was not until the work of Rabin and Klick (18) that the simplicity of the color center formation at these temperatures was shown. The results of their work and others (19, 20, 21, 22) on sodium chloride showed that F-center production can be broken into two stages, the primary stage and the secondary stage (some investigators report three stages). In the primary stage in which the F-center concentration nearly saturates, the rate of production of F-centers is dependent upon extrinsic factors and the process is assumed to be electron capture by existing halide ion vacancies, whose concentration is strongly affected by extrinsic factors (23, 24). The secondary stage is characterized by a lower production rate, which does not seem to show saturation behavior, and is assumed to be caused by the production of new halide ion vacancies followed by electron capture to produce F-centers. This process, while

apparently affected by the dislocation content (22, 23) of the crystal is not as strongly affected by extrinsic factors as the primary stage (19, 21).

The third stage, which is reported by some investigators, is reported after long irradiations and appears to be due to defects being produced with a non-uniform distribution and may represent defect formation in regions of radiation induced lattice distortion, which may account for the slightly different bleaching and annealing behavior observed for these defects (25).

Since the rate of formation of the various defects can be expected to have some relation to the form of the defects, considerable effort has been expended in determining the relationships in these formation rates. For example, the rate of M center formation has been shown to vary as the square of the F center concentration (26, 27). Attempts to show other relationships have shown some success, but a complete relationship between the various defects appearing has not been achieved (28).

Since some of the defects formed at low temperatures are not stable at room temperature, apparently converting to other defects (28, 29), it is possible that an understanding of the defect formation at room temperature can be enhanced if a good understanding of the low temperature formation rates and mechanisms can be found. Allowance for the conversion of these unstable defects to stable defects may be the key point now missing. It is not impossible, however, that the mechanism may be entirely different at room temperature than it is at low temperature

in spite of the fact that this would not be as aesthetically pleasing. In short, the extremely complicated manner of growth of absorption peaks at room temperature will require a considerable additional amount of work before it is understood and an understanding may not be attained until the low temperature mechanisms are better understood.

While the identification of absorption bands in an irradiated material is quite simple, the identification of defect creating the absorption is quite difficult. A two dimensional representation of recent identifications for the defects thought to be causing several of the absorption bands frequently observed in alkali halides are shown in Figure 3 (27, 30).

The F center is generally believed to consist of an electron trapped at a negative ion vacancy. The electron is shared equally by the six neighboring alkali ions and is concentrated to a large extent in the vacancy. The electron may be excited from its ground state to an excited bound state by the absorption of a visible photon (e.g., 2.30 eV in KCl at 77°K). This transition may be considered as analogous to the 1S→2P transition of the hydrogen atom. The F center is thermally stable in most alkali halide crystals at room temperature and up to temperatures approaching 250°C in some alkali halides.

The M center is thought to consist of two electrons trapped at two nearest neighbor negative ion vacancies or may be thought of as two nearest neighbor F centers. The absorption band associated with the M center lies toward longer wavelengths than that of the F center (e.g., 1.55 eV in KCl at 77°K). The transition giving rise to this absorption is

Figure 3. Two dimensional representation of some proposed crystalline defects in alkali halides

Key: □ vacancy
e captured electron
h captured hole

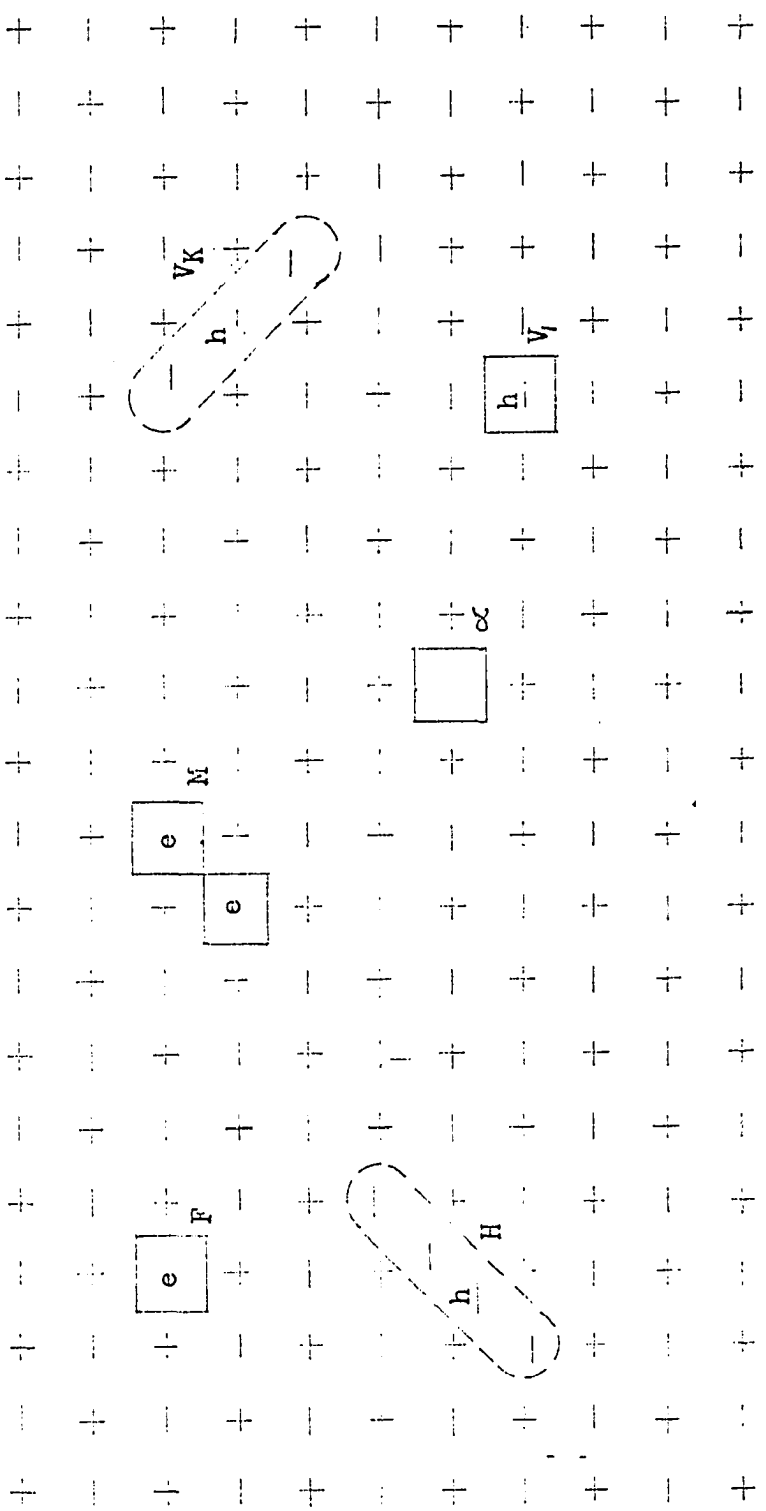
V_K
h
V_I
h
α
M
e
e
F
e
H
h

believed to be analogous to the $(1S\sigma)^2 \rightarrow (1S\sigma 2P\sigma)$ transition of the hydrogen molecule. This center is less stable than the F center thermally, but exists up to temperatures in the neighborhood of 100°C in some alkali halides.

The V_K center consists of a hole trapped at a halide ion in the perfect crystal. That is, it does not involve a defect near it. As is indicated in Figure 3, two neighboring halide ions share the hole and are pulled together slightly by the interaction. This center may be thought of chemically as being a substitutional halogen atom. These centers are stable only at low temperatures (between -140°C and -50°C in KCl) but could be an intermediate stage in defect formation at any temperature. The maximum temperature at which the V_K centers are stable is determined by the impurity content of the crystal. The optical absorption band arising from this center occurs at 3.40 eV in "pure" KCl at 77°K and results from a transition that is analogous to $np\sigma_g \rightarrow np\sigma_u$ in the Cl_2^- molecule.

The H center consists of a hole trapped at an interstitial halide ion. As indicated in Figure 3, this hole is shared by three substitutional halide ions plus the interstitial ion. This may be described as a Cl_2^- ion which has been substituted for a single Cl^- ion. Chemically this center resembles an interstitial halogen atom. This center is stable only at temperatures below about 40°K but again may play an intermediate role at other temperatures. The H center introduces an absorption band at 3.70 eV in KCl at 4.2°K. The optical absorption may be thought of as arising from the transition $np\sigma_g \rightarrow np\sigma_u$ of a Cl_2^-

molecule. Although this transition is the same as for the V_K center, the change in the internuclear distances in the H center from that in the V_K center modifies the position of the absorption band.

The α center, as shown in Figure 3, arises from a negative ion vacancy. It should be noted that this is simply an ionized F center. The absorption arising from this center lies in the ultraviolet portion of the spectrum to slightly longer wavelengths than the fundamental absorption of the host crystal (e.g., 7.0 eV in KCl). The α center absorption is seen only at temperatures below about 100°K. A similar perturbation of the fundamental lattice excitation occurs in the neighborhood of the F center. The trapped electron compensates somewhat for the absence of the halide ion, so the perturbation is not so great and gives rise to the β band at 7.45 eV in KCl.

Several mechanisms have been suggested for the formation of defects due to exposure of alkali halide crystals to ionizing radiation. Examination of these mechanisms shows three basic mechanisms for producing halide ion lattice defects, the predominantly observed type of defect, with many modifications existing for each basic mechanism.

One type, which was suggested by Seitz (31), is characterized by the single ionization of a halide ion. In this process the energy released when the free atom recombines with an electron to reproduce an ion is converted into lattice vibrations and if this occurs near a dislocation jog or other lattice disruption which would trap an ion if it were released from its lattice site, a highly excited point might be produced from which either a positive or negative ion vacancy might

result by the movement of an ion. By this process the formation of positive and negative ion vacancies would be produced, in approximately equal numbers so that the dislocation line or other defect region maintains a neutral charge. A correlation between the number of dislocations and the efficiency of the crystal in defect formation would be expected.

A second type of mechanism, which was introduced by Varley, is based on the idea that a halide ion can be multiply ionized. Varley (32) suggested that a reasonable probability might exist for the double ionization of a halide ion. The halide ion would then have a positive charge. Being surrounded by six positive nearest neighbors, it would be in an unstable equilibrium, and would easily be ejected into an interstitial position where it could be expected to regain one or both electrons quite rapidly. This type of mechanism is more probable if Varley's proposal is modified to allow for the double ionization resulting from the well known Auger process, which involves first the removal of an electron from an inner shell with the removal of the second due to the x-ray produced when outer orbit electrons fall into lower orbits to re-establish equilibrium in the molecule. The probability of this process is much higher than for the direct double ionization of the halide ion (33).

The third type of mechanism, which has been proposed specifically to explain the absorption peaks produced by liquid helium temperature irradiation of the alkali halides, is characterized by the assumption that defect production is the result of the single ionization of two halide ions which occupy nearest neighbor positions. Mechanisms of

this type have been suggested by both Klick (34) and Williams (35). Klick has suggested that two adjacent halide ions which are ionized nearly simultaneously will form a neutral halogen molecule, which will be localized at one halide ion site. This would then form a vacancy and a neutral halide molecule substituted for a halide ion. Williams modifies this by suggesting that two atoms formed in the ionization will move toward neighboring halide ions. This motion would result from an ion-induced dipole force. In short, the tendency would be for one of the neutral atoms to form a negative halogen molecule. When the changes in the coulomb energy due to the formation of the negative molecule are considered, it appears that sufficient momentum is imparted to the halogen molecule to produce a series of "billiard ball" collisions of the ion cores. This leads to a separation of the negative halogen molecule and the vacancy (i.e., the molecule retains one vacancy site and separates from the other vacancy site). The second atom can move away from the vacancy by hole motion. As a result, α , H and V_K centers are formed. The resulting color centers would depend upon which of these defects captured the electrons released by the ionization.

Considerable effort has been spent on attempts to determine which of the mechanisms or which combination of mechanisms seems most likely to be the predominant form in defect production. A recent examination of the problem by Ritz appears to shed more light on the problem than most to date. Ritz (36) has made a systematic study of the efficiency (energy required to produce one defect) for F center formation at liquid helium temperature by irradiation fields which produce differing ionization

densities.

Before examining the experimental findings, an examination of the variation of efficiency with ionization density for each of the proposed mechanisms will be beneficial. If the mechanism is one of single ionization events, such as suggested by Seitz, one would expect the efficiency to be highest for high energy electrons--low ionization density--(of the order of 2 Mev as opposed to electrons of a few Kev energy). This change in efficiency is in main due to the increasing probability of back reaction for the ionization process as ionization density increases.

If multiple ionization processes on a single ion are the predominant mechanism, the calculations of Durap and Platzman (37) show that the energy to form an F center also goes up as the electron energy decreases (i.e., the efficiency decreases as the ionization density increases), as was the case for the single ionization mechanism.

If the mechanism suggested by Klick and Williams in which the ionization of two adjacent halide ions is assumed to be the defect production mechanism, the probability and efficiency of this process increases with increasing ionization density since the probability of two nearest neighbor halide ions both being ionized increases with increasing ionization density. Note that the stopping power for a photo electron arising from a lower energy x-ray is much higher than that from a higher energy photon.

Examination of Ritz's results shows several points:

1. The energy to form an F center has the same qualitative behavior for all the alkali halides studied.

2. The efficiency of F center formation shows a definite increase as the ionization density increases.

3. As the ionization density increases beyond that due to 50 Kev x-ray, the efficiency decreases.

From these points it becomes apparent that the mechanisms proposed by Seitz and Varley do not show the proper energy dependence and are in all probability not the low temperature defect production mechanisms effective in the alkali halides.

The slight decrease in efficiency at the high end of the ionization density scale needs explanation, which Ritz provides, by pointing out that at these high ionization densities the production of three nearest neighbor ionizations becomes possible, resulting in the production of more complex defects with the resulting decrease in efficiency for F center production.

Recent work on comparisons of lattice parameter change against density change (38, 39) have given additional emphasis to a recent modification (40, 41) of the mechanism proposed by Klick and Williams.

The modification involves assuming that electrons can recombine with the holes captured at H and/or V_K centers, with the possibility of either a radiation releasing capture which returns the lattice to normal, or a non-radiative capture for which the energy released by the recombination is sufficient for displacement of a halogen ion in a [110] direction in the lattice if the energy is shared unequally due to lattice interaction by the halogen ions at which the hole was originally captured. The halogen ion thus expelled can either form a Frenkel defect

or by collision with an alkali ion cause a [110] displacement of the alkali ion with resultant Schottky defect formation. Additional considerations indicate that this mechanism can explain the temperature dependence of F center formation (28, 42), the luminescence peak observed at ~190°K for samples irradiated at liquid helium temperature (43) and the observed impurity dependence of F center formation rates (41).

Defect Interactions

While the defect spectrum observed at liquid helium temperature following liquid helium temperature irradiation is quite simple, the defect spectrum observed at higher temperatures becomes quite different. The changes in absorption behavior at higher temperatures are generally thought to be due to defect interaction and annealing.

Examination of the F center absorption peak shows behavior which has been associated with defect interaction and annealing (44).

Observation of the F center concentration as a function of irradiation dose rate and temperature shows complex behavior which is typical of the behavior of most defects (45, 46). In general, higher temperatures tend to favor the formation of more complex defects with an associated decrease in the F center concentration while increasing the dose rate favors complex defect breakup, with the associated increase in F center concentration. The concentration of F centers shows a non-linear relationship to the dose rate, with the concentration showing a more than linear dependence upon the dose rate (45, 47). The tendency toward simpler defects at higher dose rates and toward more complex

defects at higher temperatures of irradiation does not hold above the stability temperature of the complex defects. Above the stability temperature complex defects break down to simpler defects, which can recombine as occurs during annealing.

CONDUCTIVITY BEHAVIOR OF NACL UNDER IRRADIATION-LITERATURE SURVEY

The extrinsic region of the conductivity versus reciprocal temperature plot can be significantly altered by irradiation, and is the region in which most of the experimental work has been carried out.

The change in conductivity observed in the extrinsic region has been shown to depend upon the type of radiation to which the sample is exposed. The work of Nelson, Sproull, and Coswell (48) showed that a room temperature exposure to reactor radiation led to a decrease in conductivity at first but an increase in conductivity for long term exposure for samples after removal from the radiation field. Examination of conductivity changes associated with gamma ray exposure for specimens removed from the radiation field shows that the conductivity decreases significantly, but that saturation of the decrease is observed which is much more rapid than that due to neutron exposure (48). As a result the behavior upon reactor exposure has been interpreted as the result of a rapid saturating decrease from gamma exposure and a long term increase due to neutron exposure (49).

Initial studies of the effect of annealing (48) were done as isochronal annealings studies. Initially relatively large heating rates (around 10°C per minute) were used, and nearly straight line, conductivity versus 1/T, behavior was observed up to about 175°C, after which deviation from linearity was observed and interpreted as annealing behavior. Later work in which lower heating rates (about 1°C per minute) were used showed more complex behavior (50).

Several interpretations of this behavior are possible (51) with

the work of Kobayashi (52) being quite thorough. By heating sodium chloride crystals after irradiation with 350 Mev protons at 2°C per minute and periodically cooling the samples to room temperature for measurements the electrical conductivity, stored energy release and color center behavior could be correlated during the annealing process.

Kobayashi has interpreted the observed behavior as follows:

1. In the first stage (room temperature to 150°C) the primary changes in the defect concentrations involve the clustering of simple defects. Complex absorption centers such as the M and N bands increase significantly, while the F band decreases, (the M band is assumed to be due to two combined F centers, while the N band is due to a combination of four F centers) (27). Examination of the conductivity of the crystal shows a sharp decrease in the conductivity in the first stage. The additional mobility of the F centers in this temperature range may account for the decrease in conductivity by depressing the positive ion vacancy level. In addition complex defects containing cation defects may also be formed in this temperature range.

2. In the second stage, 150°C to 200°C, the conductivity increases. This may be interpreted by noting that while the concentrations of the bands containing F centers and combinations of F centers are decreasing, the F center coagulation band at 578 mu is rapidly increasing, indicating that the F centers are not being released to the crystal but are forming into larger less effective trapping sites, while the V bands, which are thought to involve positive

ion vacancies and complexes of them (53) are breaking up to produce positive ion vacancies and as a result, the conductivity increases in this temperature range.

3. In the third stage, (200-250°C), the F center coagulation centers are no longer stable and break up to produce F centers which are again available to combine with cation-vacancies to form neutral divacancy pairs. As a result, the conductivity again decreases.

4. In the final stage the crystal begins to return to normal, as the excess F center contribution due to the break up of the coagulation centers finally disappears, and the annealing of all complex defects is completed.

More recent writers have placed emphasis on electron and hole capture effects on conductivity. The conductivity changes of crystals doped with divalent cation impurities have been interpreted on the basis of electron capture by the divalent atoms (54, 55), reducing divalent impurities to the monovalent state, with the resultant decrease in the extrinsic contribution to the conductivity possibly due to dipolon (neutral divacancy pair) formation (56). The formation of dipolons would also explain the lack of F center clustering observed for crystals containing high concentrations of divalent cations. Dipolon formation would be expected to decrease the conductivity of the crystal.

Capture of virtual positive charge holes by the virtual negatively charged positive ion vacancies is also possible and may play a role in conductivity changes. Support for this view can be found in the interpretation of paramagnetic resonance by some investigators. Among the

resonance peaks observed is one which exhibits the behavior which would be anticipated for a halide ion molecule (X_2^-) captured at a cation vacancy (57). This would favor anion vacancy formation and a decrease in the positive ion vacancy concentration, which would be compatible with observed conductivity changes (58) under gamma irradiation.

Additional insight into the effect of radiation on ionic conductivity has been offered by isothermal annealing experiments following x-ray irradiation of KCl (59, 60).

In these experiments it was found that isothermal annealing following room temperature irradiations led to a rapid increase in the conductivity of the crystal followed by an asymptotic decrease. The time dependence for the decrease in conductivity was compatible with the interpretation of the conductivity changes during annealing experiments in which potassium chloride crystals were quenched in liquid nitrogen from temperatures near the melting point of KCl. Interpretation of these results on the basis of the assumption that the diffusion of the chloride ion vacancy controls the observed behavior leads to the conclusion that the excess chloride ion vacancies are diffusing to and annihilating at "subgrain mosaic blocks" approximately 10^{-5} cm on a side for the quenching experiments (61-62) and somewhat less for the irradiated specimens (60). The presence of block boundaries has recently been shown to be related to the formation of grains in sodium chloride (62) crystals.

A different approach in determining the effect of radiation on conductivity is of the type used by Hacke (63), who measured the effect of x-irradiation on the ionic conductivity of NaCl, with the measurements

being made during irradiation. The results of his work are shown in Figure 4.

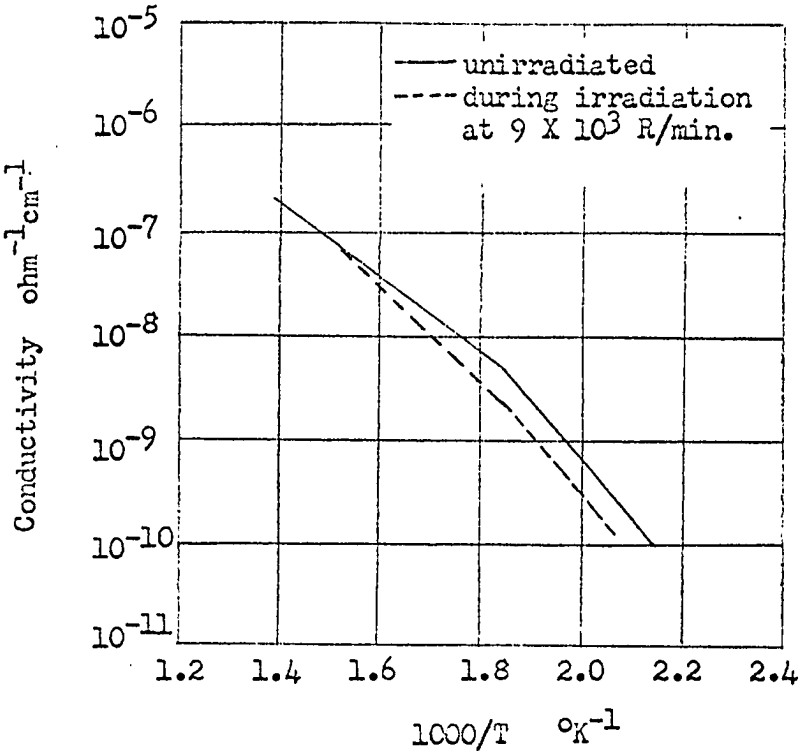

Figure 4. Conductivity of sodium chloride crystal as a function of reciprocal temperature with and without radiation

It was pointed out by Hacke that during the irradiation the ionic conductivity was influenced only in the extrinsic region, where it lowered the conductivity. At lower irradiation temperatures (in the associated region), the activation energy was not altered, however, at the higher temperatures (in the extrinsic region) examined it was increased.

No explanation of the behavior upon irradiation is given in the original article, however, the effect of the irradiation on the conductivity observed by Hacke has been interpreted on the assumption

that a solubility product type relationship exists between positive ion vacancy concentration and the negative ion vacancy concentration (64). It can be argued that the effect of the irradiation on the positive ion sublattice will be unimportant until some very low temperature is reached at which the positive ions will be immobile. At temperatures above the immobility point the positive ion sublattice can respond quite rapidly compared to the negative ion sublattice. As a result, the positive ion vacancy concentration could be expected to adjust to provide an equilibrium concentration of vacancies such that the free energy of the system will be a minimum. This condition can be expected to be expressed by the solubility product-type relationship: $[C_+]\,[C_-]$ = constant (where $[C_+]$ and $[C_-]$ are the concentrations of positive and negative ion vacancies respectively) so long as one of the species is able to adjust its equilibrium concentration. In sodium chloride this would have the effect of depressing the conductivity as the more mobile cation vacancy concentration is reduced by the increase of the concentration of the less mobile anion vacancies. No experimental evidence other than the previously mentioned observation that gamma irradiation does produce anion vacancies and the conductivity during and after gamma irradiation is decreased has been advanced for this mechanism.

EXPERIMENTAL APPARATUS AND PROCEDURE

Experimental Outline

Nearly all of the radiation damage mechanisms which have been proposed to explain the effect of ionizing radiation on the alkali halides and the explanations for the color centers formed during irradiation of alkali halide materials involve the formation of anion vacancies and their interactions after formation. Recent work on the polarization behavior (4) of sodium chloride has suggested that the long time constant polarization current is proportional to the anion vacancy concentration in the material. If these experimental interpretations are compatible, then the polarization current observed during irradiation of sodium chloride should be higher than that observed for the unirradiated material. Since the steady state d.c. conductivity of sodium chloride has been shown to be proportional to the cation vacancy concentration for unirradiated sodium chloride, it should also be possible to monitor the concentration of the cation vacancies during irradiation if the photo induced current is not too large.

As a result, the experimental apparatus needed to provide steady state d.c. conductivity and polarization measurements for unirradiated sodium chloride single crystal material and for the same material after equilibrium had been achieved during irradiation was constructed. The objective of this experiment was to collect the data necessary to determine the steady state d.c. conductivity and the additional long time constant conductivity, the blocked conductivity, which appears after a change of the polarity of the applied electric field, in order to

provide a more complete knowledge of the behavior of the electrical conductivity of alkali halide materials during irradiation.

Experimental Apparatus and Materials

Specimen preparation

The specimen used in the experiment was prepared by cleaving an approximate 2 mm length from the center of a Harshaw sodium chloride ingot 12.5 mm in diameter by 5 mm in length, thereby providing fresh contact faces on the specimen. Electrical contacts for the specimen were prepared as follows:

1. One surface of the crystal was polished using number 600 silicon carbide paper. The other surface was protected by a gold foil during the polishing.
2. The polished surface was painted with Englehard number 05-X liquid platinum bright and baked in a furnace for 30 minutes at 285°C, with the opposite face resting on a gold foil.
3. The second contact face was polished using number 600 silicon carbide paper. The finished contact surface was protected with a gold foil.
4. The second contact face was painted with platinum paint to provide a guard circuit configuration (4).
5. The crystal was placed on a gold foil in the furnace and baked for 30 minutes at 285°C followed by 30 minutes at 500°C.

In order to provide as uniform a thermal history as possible, the specimen was annealed by heating at 500°C for 4 hours and cooling at

15° per hour to a temperature below the temperature at which the experimental data was collected before each irradiation run. The conductivity returned to the pre-irradiation value for every run except run number 3, for which the conductivity following the anneal was approximately 20% higher than the original pre-irradiation value. As a result, the data from run number 3 was multiplied by the ratio of the original pre-irradiated data to the value prior to run number 3.

Specimen holder

Since a maximum irradiation container diameter of four inches can be placed in the radiation field for the facility used, it was necessary to design a compact specimen holder suitable for high resistance measurement with provision for specimen temperature variation and control. A cross section of the sample holder used for this experiment is shown in Figure 5 and a photograph in Figure 6a. The heater consisted of 15 inches of No. 28 chrome Alumel wire with No. 20 nickel leads attached. Other parts are identified in the figure. Thermocouple output accuracy was checked by determining the melting point of 99.999% purity lead specimens from cooling curves for samples weighing approximately 10 grams placed in quartz dishes in the conductivity apparatus in place of the specimen. Less than 1% error was observed for each of three trials.

Specimen environment

The irradiation chamber used in this experiment is shown in Figure 6b. The specimen environment used during the experiment was obtained by evacuating the irradiation chamber to a pressure of approximately 1

Figure 5. Conductivity apparatus

1. 1/16" steel rod
2. 21 mm OD quartz tubing
3. 15 mm OD quartz tubing
4. steel spring
5. stainless steel end plates
6. iron-constantan control thermocouple
7. brass washer
8. conductivity leads
9. 3 mil. platinum foils
10. heater wires (see text)
11. measuring thermocouple
12. 9 mm OD vycor tubing
13. stainless steel contact plates
14. asbestos insulation

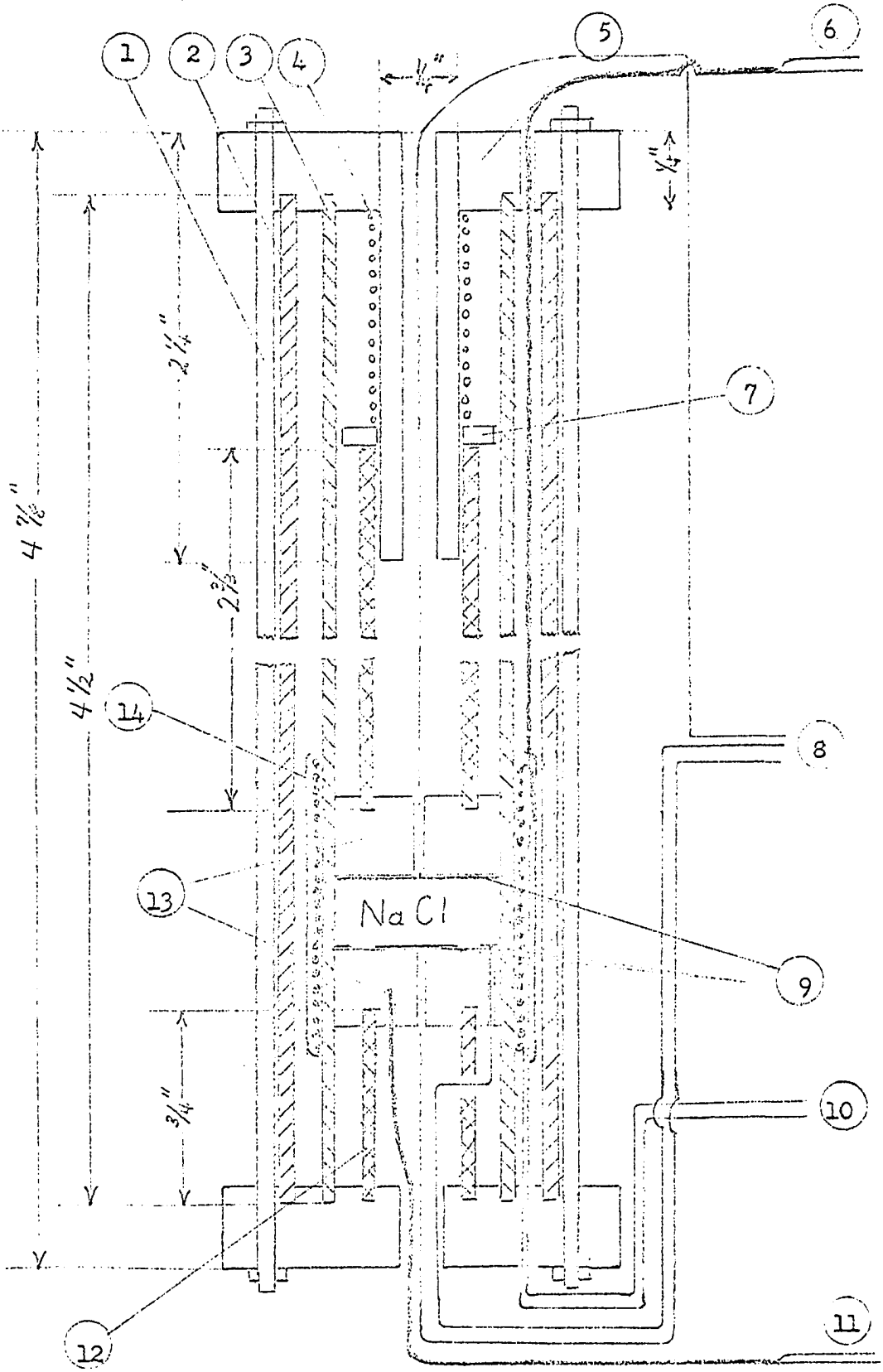
1
2
3
4
5
6
7
8
9
10
11
12
13
14
NaCl
4 7/8"
4 1/2"
2 1/4"
2 3/8"
3/4"
1/4"
1/4"

Figure 6a. Photograph of conductivity apparatus

Figure 6b. Photograph of irradiation chamber

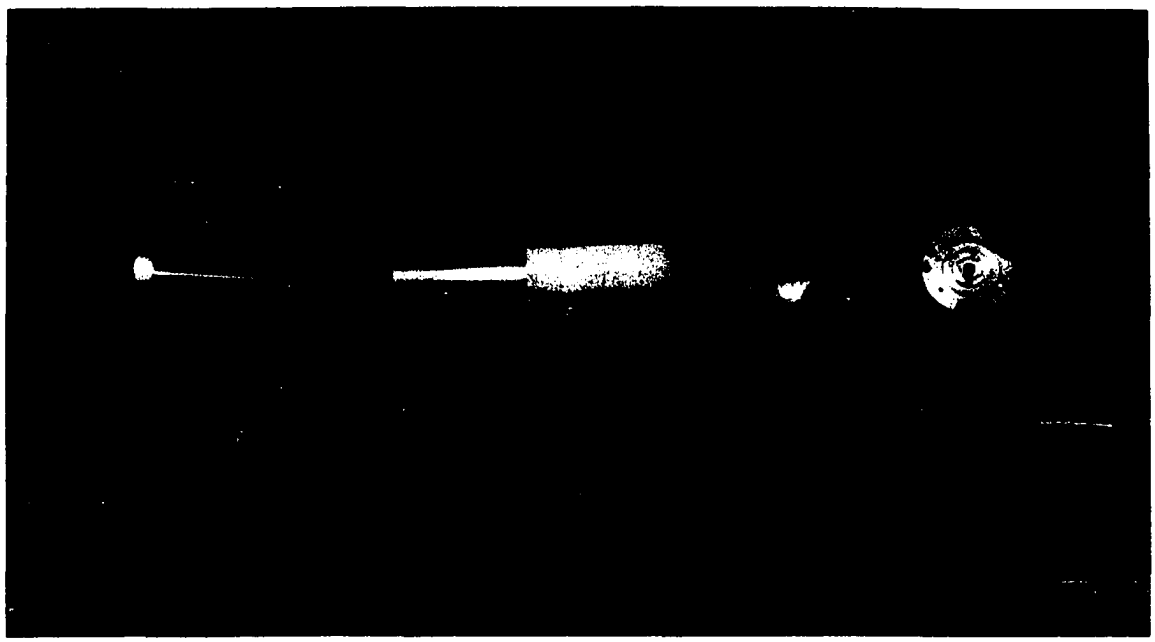

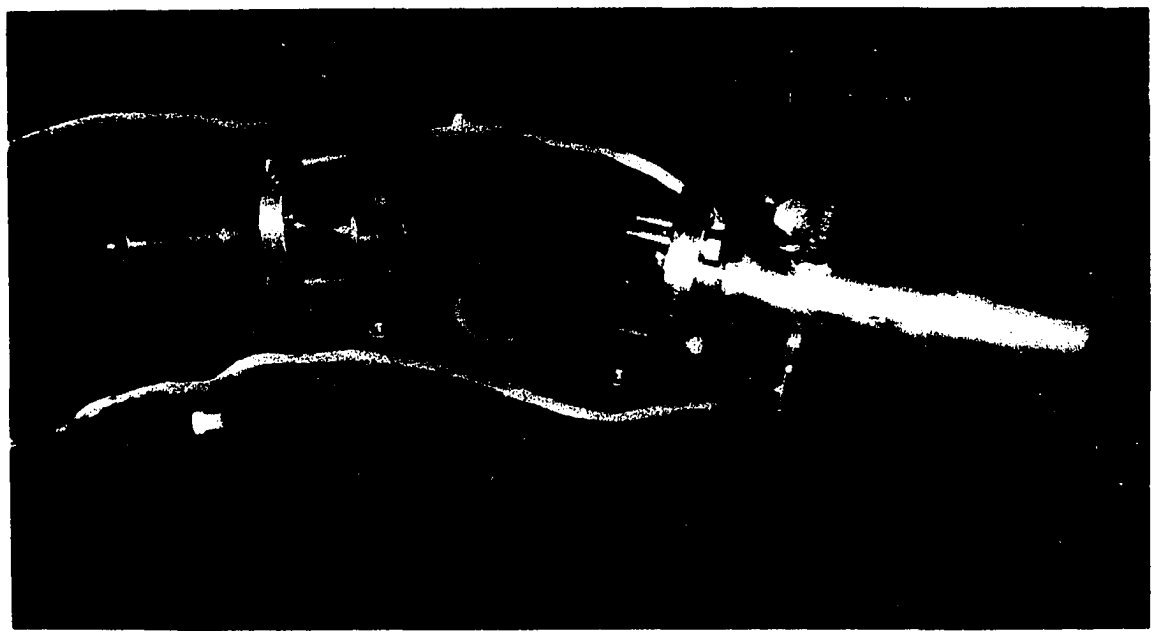

micron, at which time the sample temperature was raised to 500°C. Pumping was continued until the pressure returned to approximately 1 micron and closing the system off from the pump showed a pressure rise of less than 1 micron per 5 minutes. The apparatus was cooled to room temperature with the vacuum pump working. The system was isolated from the pump and filled to approximately 4 psig with commercial dry purified helium.

Irradiation facility

A cutaway view of the irradiation facility is shown in Figure 7. The radiation source consisted of approximately 5,000 curies of cobalt-60. The irradiation chamber was attached, as is shown in the figure for a similar irradiation container, below a shield plug which is driven up and down by an electric motor through a rack and pinion drive. Vertical positioning is achieved by observing a fixed pointer relative to a vertical scale on the moving rack (the positioning mechanism is above the portion of the facility shown in the figure). Dose rate variation is achieved by moving the sources in toward the sample container from the out position shown in the figure by rotation of the hand driven wheel shown just below table height. The wheel is fitted with a vernier and scale for use in positioning the sources.

Measuring apparatus

A block diagram of the measuring equipment is shown in Figure 8. Lead designations refer to the leads shown in Figure 5.

Temperature control was achieved by use of a Leeds and Northrup

Figure 7. Co-60 irradiation facility (scale approximately 10 to 1)

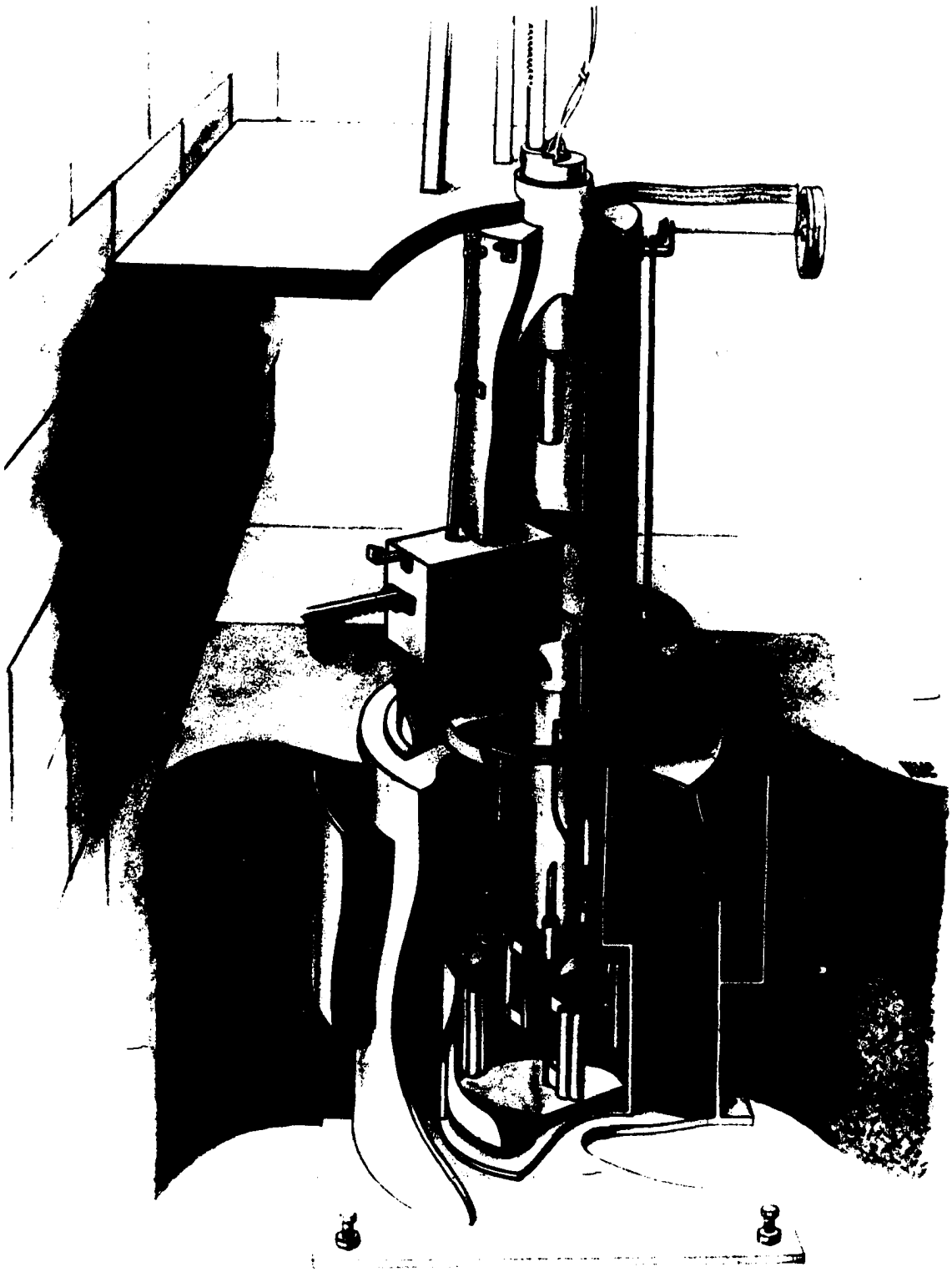

Figure 8. Block diagram of apparatus for conductivity measurements

Key: VTVM #1 guard circuit null meter
VTVM #2 crystal current null meter

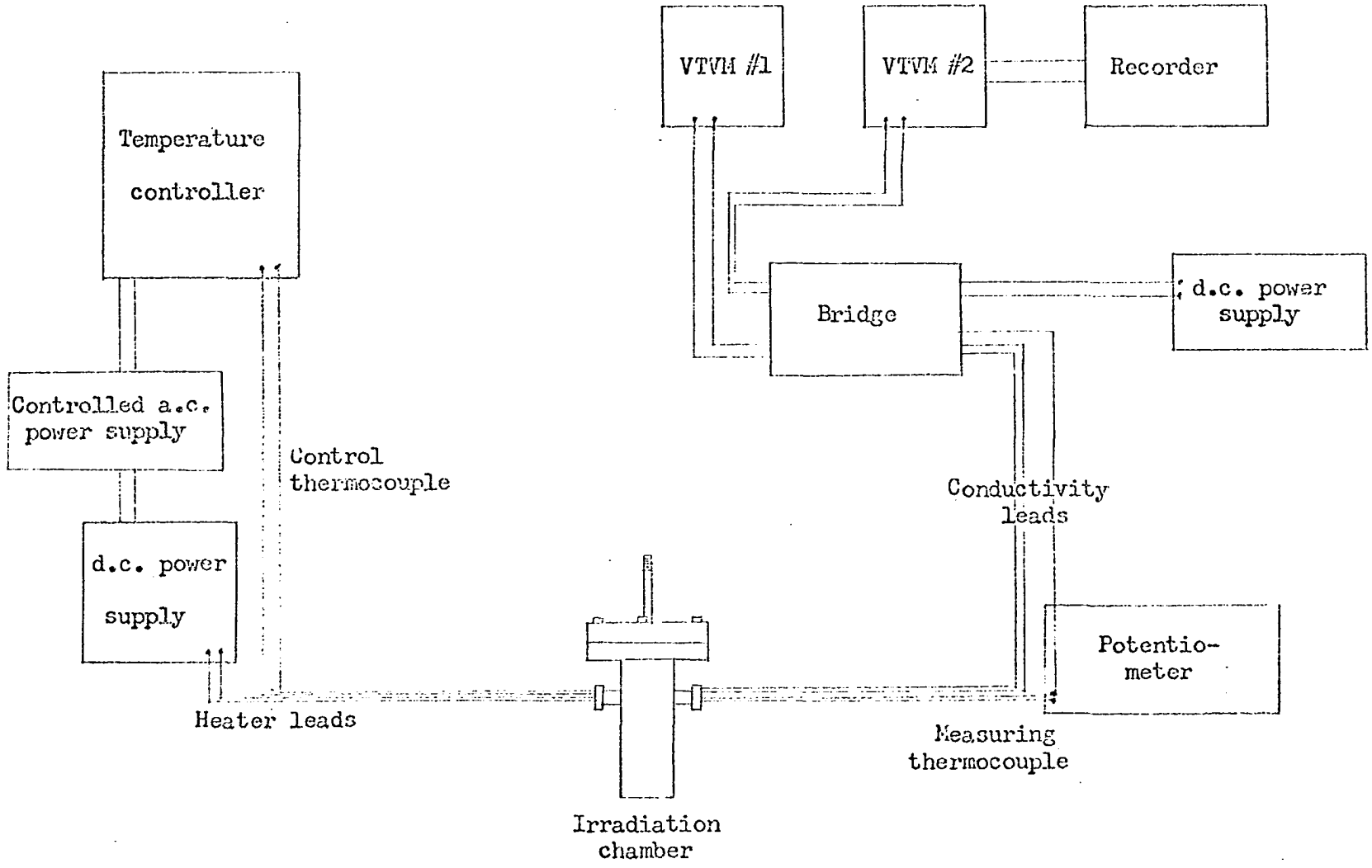
VTVM #1
VTVM #2
Recorder
Temperature controller
Bridge
d.c. power supply
Controlled a.c. power supply
Control thermocouple
Conductivity leads
d.c. power supply
Potentio-meter
Heater leads
Measuring thermocouple
Irradiation chamber

"Speedomax H" recorder and "Cat 60" three mode controller which varied the voltage output from a Leeds and Northrup No. 10915-50 silicon controlled rectifier power package. The a.c. output from the silicon controlled rectifier package was used as the input to a model D-612T Electro d.c. power supply which provided the power for the conductivity apparatus heater. Temperature measurement was achieved by means of a Honeywell model 2745 potentiometer. One leg of the measuring thermocouple was used to provide one lead for the measuring circuit. Temperature variation was observed to be less than $\pm$ 0.2°C.

Conductivity values were calculated from measured physical dimensions and resistance measurements for the crystal. The crystal resistance was determined by use of a modified Wheatstone bridge. A schematic for the bridge is shown in Figure 12 in the Appendix. Hewelett-Packard model 412A vacuum tube voltmeters were used for null measurements. The d.c. voltage for the bridge was supplied by a model 711A Hewelett-Packard d.c. power supply. Time dependent conductivity measurements after polarity changes were obtained by recording the out of balance voltage for the crystal circuit of the bridge. A model G-11A Varian recorder was used for recording the out of balance voltage.

The crystal thickness was measured with a micrometer. The specimen was protected from contamination during the measurements by 3 mill platinum foils.

Procedure

Resistance measurements for the unirradiated material were taken with the following sequence of steps.

1. The temperature controller selector switch was placed on manual and the temperature for the test was obtained by varying the d.c. power supply output voltage with the controller manually set such that the silicon controlled rectifier gave 115 volts a.c. output. Once the temperature was close to the desired temperature, the controller was switched to automatic. Thirty minutes were allowed for temperature stabilization.

2. The d.c. power supply was set to 30 volts d.c. and approximately 1 hour was allowed for the conductivity to reach a constant value. This conductivity value was designated the steady state d.c. conductivity.

3. The polarity of the d.c. voltage across the crystal was reversed and the out of balance voltage recorded as a function of time after polarity reversal.

The process was repeated for the measurements during irradiation. The specimen was lowered into the radiation field immediately after the crystal reached the test temperature. Times longer than 1 hour were required to reach steady state for the lower temperatures during irradiation.

The dose rates used in this experiment were determined by removing the crystal from the conductivity apparatus and replacing it with a glass vial containing Fricke dosimetry solution. The apparatus was assembled and lowered into the irradiation position for exposure. Change in absorption coefficient for the solution was determined with a Beckman DU spectrophotometer. The dose rate is know with an accuracy of $\pm$ 4%.

RESULTS AND DISCUSSION

Conductivity of Unirradiated Specimen

The conductivity of the single crystal sodium chloride used in this experiment is shown as a function of reciprocal temperature in Figure 9. The activation energies for the different regions and absolute magnitude of the conductivity are close to those found in the literature. The value of 1.67 ev for the intrinsic region activation energy is in good agreement with the value, 1.66 ev, found in the literature (4, 5). The value for the extrinsic conductivity region, 0.80 ev, is in good agreement with the value, 0.79 ev, given in the literature (5). The position of the "knee" ($1000/T \sim 1.41^{\circ}K^{-1}$, $\sigma \sim 7.5 \times 10^{-6}$ $ohm^{-1}cm^{-1}$) is at a somewhat higher temperature and conductivity than usually given for Harshaw "pure" sodium chloride crystals in the literature ($1000/T \sim 1.4^{\circ}K^{-1}$, $\sigma \sim 6 \times 10^{-8}$ $ohm^{-1}cm^{-1}$) (4, 5), although the variation is small. It seems likely that some impurities may have been introduced during the cleaving and contact production processes. The activation energy found for the association region, 1.07 ev, is within the range of values reported in the literature, 0.95-1.1 ev, (5). The activation energy determined from the blocked conductivity data, 1.01 ev, is close to that found previously, 1.08 ev, (4) and also is within the spread of experimental values found for the motion of the anion vacancy in diffusion studies, 0.9-1.1 ev, (11, 12, 13) and is reasonably close to that found by theoretical calculation, $\sim$ 1.2 ev, (65).

Figure 9. Conductivity of sodium chloride versus reciprocal temperature before irradiation and after irradiation runs were completed and the sample was annealed at 500°C for 4 hours.

Key
- x pre-irradiation steady state d.c. conductivity
- . post-irradiation steady state d.c. conductivity
- ⊗ pre-irradiation blocked conductivity
- ⊙ post-irradiation blocked conductivity

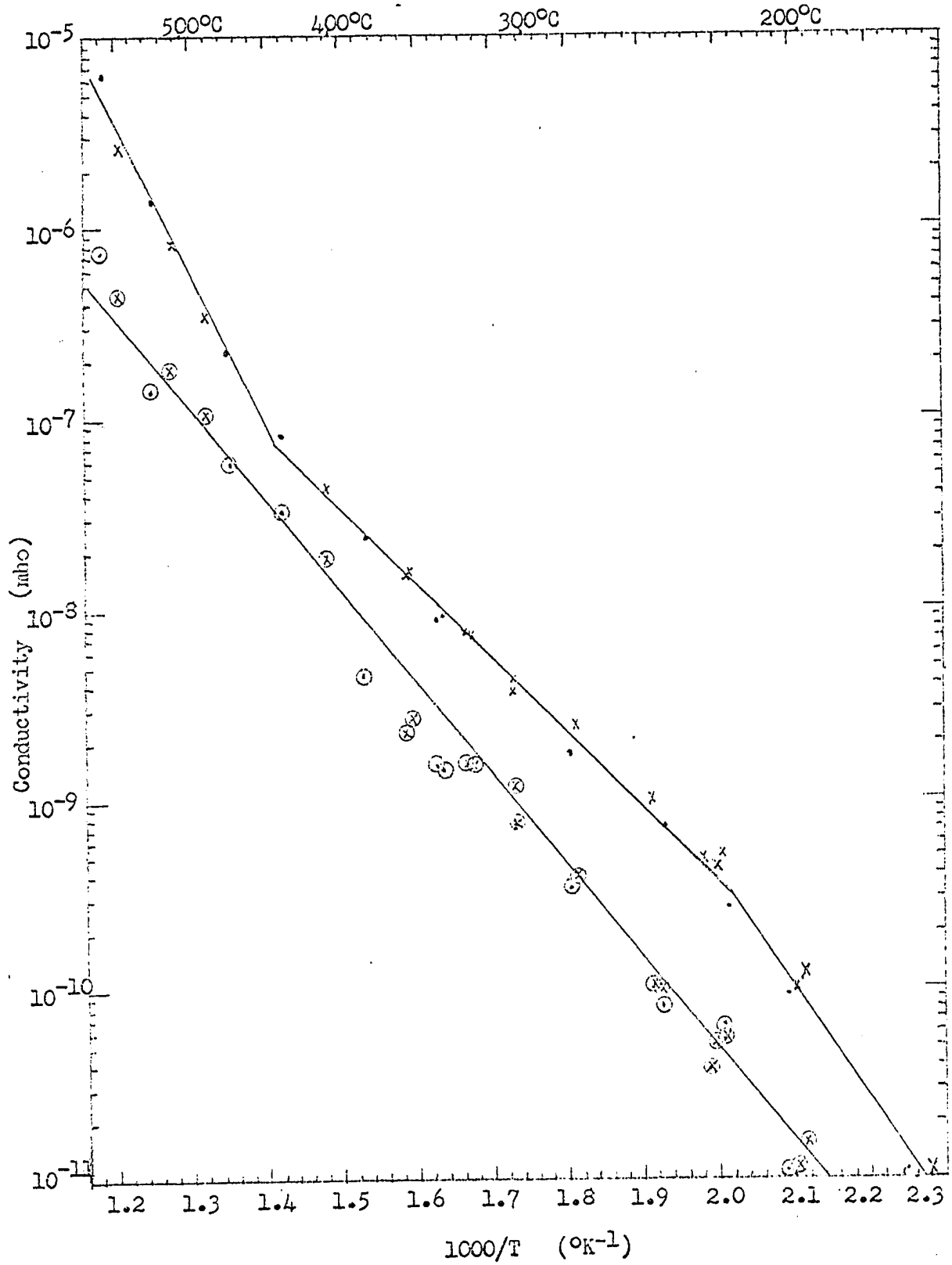
500°C
400°C
300°C
200°C
10^{-5}
10^{-6}
10^{-7}
10^{-8}
10^{-9}
10^{-10}
10^{-11}
Conductivity (mho)
1.2
1.3
1.4
1.5
1.6
1.7
1.8
1.9
2.0
2.1
2.2
2.3
1000/T (°K-1)

Conductivity During Irradiation

Steady state d.c. conductivity

The steady state d.c. conductivity during irradiation is shown in Figure 10. The unirradiated conductivity behavior is shown as a dashed line for comparison. The conductivity at all dose rates examined is less than for the unirradiated material. Increased dose rates decrease the activation energy found. This behavior can be explained if it is assumed that the observed behavior is strongly affected by two factors.

First, during the irradiation halide ion vacancies are being formed. The production of a halide ion vacancy would seem to require that interstitials must be formed during irradiation. Since interstitials can be charged, their motion could produce conduction. The activation energies found for anion interstitials from theoretical calculations for sodium chloride fall within the range 0.26 ev to 0.73 ev (66, 67). In addition, if cation vacancies are produced during irradiation, the cation interstitials could also add to the conduction. Since the activation energies for the motion of both anion and cation interstitials are found to be less than that associated with the sodium ion vacancy, it is possible that the decrease in the observed activation energy for the d.c. steady state conductivity as dose rate increases may be due to increasing conduction by interstitials, the concentration of which would be expected to increase with increasing dose rate.

The presence of interstitials due to irradiation has been reported in optical absorption studies following irradiations at liquid helium temperature for samples examined at liquid helium temperature. Observation

Figure 10. Steady state d.c. conductivity versus reciprocal temperature for unirradiated sodium chloride and for sodium chloride during gamma ray irradiation at gamma ray dose rates of 2.73×10^3 rad/min, 5.46×10^3 rad/min and 1.09×10^4 rad/min

Key
- ------ unirradiated
- ⊙ 2.73×10^3 rad/min
- x 5.46×10^3 rad/min
- \+ 1.09×10^4 rad/min

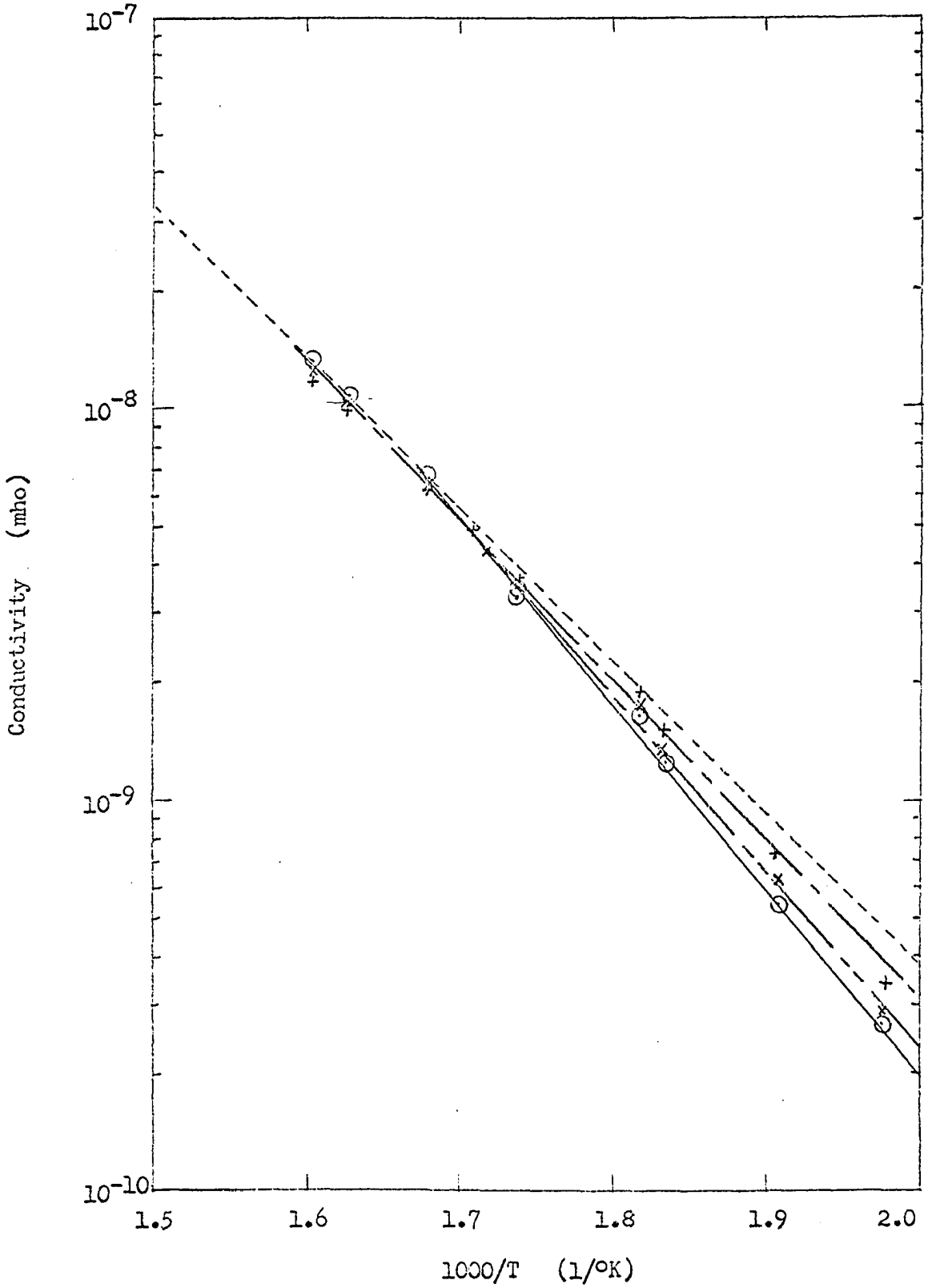
10^{-7}
10^{-8}
10^{-9}
10^{-10}
Conductivity (mho)
1.5
1.6
1.7
1.8
1.9
2.0
1000/T (1/°K)

of the absorption spectrum for the irradiated crystals during heating to room temperature shows a decreased absorption at the absorption wavelength thought to be due to interstitials and an increase in absorption at a wavelength thought to be due to coagulation of interstitials, and loss of some interstitials by recombination with vacancies (68).

Photo electrons and holes can also be expected to be produced and contribute as a part of a total photo-induced steady state conductivity.

The second factor assumed to be occuring is a decrease in conductivity due to a decrease in the cation vacancy concentration. This decrease may be due to any one of several postulated mechanisms, or a combination of these effects. Suggested mechanisms include the conversion of divalent impurities to monovalent ions with the resulting loss of cation vacancies in the extrinsic region (54, 55), the possibility that V_1 centers consist of neutral anions trapped in cation vacancies removing the cation vacancy as a conduction entity (53, 58), and the possibility of a decrease in the cation vacancy concentration due to dipolon (neutral vacancy pairs) formation between cation vacancies and radiation induced anion vacancies (56). The defects assumed to be causing the decrease in conductivity in all three mechanisms are thought to be unstable at the temperatures used in these experiments (69). The concentration of these defects will be set by the rates of production and of destruction. The rate of production can be expected to be proportional to dose rate, and increased dose rate should lead to greater concentrations of conductivity reducing defects. As a result, increased dose rates should lead to lower cation vacancy conduction

values.

If a decrease in cation vacancy concentration by radiation is assumed to be present, a decrease in the rate of cation self diffusion should be expected during irradiation. A decrease in the cation self diffusion rate during x-irradiation has been observed at temperatures up to approximately 550°C (70).

If these two factors (conduction by photo-induced carriers and depression of the cation conduction) are assumed to be active, the observed behavior can be explained as follows.

At any given temperature the conduction by cation vacancies decreases, while conduction by photo-induced carriers increases with increasing dose rate. The lower activation energy for the photo-induced carriers makes the photo-induced current more important at lower temperatures, causing the increase in conductivity observed for the dose rates 1.09×10^4 rad/hr and 5.46×10^3 rad/hr above the value observed for the 2.73×10^3 rad/hr irradiation at the lower temperatures examined. At the higher temperatures examined, the photo current represents a much smaller addition to the total conduction and the decrease in conduction due to the decrease in the cation vacancy concentration becomes apparent.

The depression observed for the cation conduction during irradiation is somewhat less than observed in previous work (63, 71) with x-irradiation for equivalent crystal pre-treatment, but this may be due to the higher efficiency for anion vacancy production by x-rays as compared to Co-60 gamma rays (20). The higher anion vacancy production efficiency for the x-rays would give a larger anion vacancy formation

rate for equal absorbed energy, leading to greater cation depression by any of the mechanisms previously discussed and less energy available for the production of other photo-induced carriers.

The possibility of exciton produced positive ion vacancies due to non-radiative capture of electrons at holes is possible as previously discussed. The lower efficiency for anion vacancy formation by Co-60 radiation compared to x-radiation may be the result of increased neutral Schottky pair formation by the exciton process during Co-60 irradiation. With fewer single anion vacancies produced, cation conduction would not be decreased as greatly for Co-60 irradiation as for x-ray irradiation of equal absorbed dose.

Blocked conductivity

The long time constant time-dependent or blocked conductivity observed during irradiation is shown in Figure 11. Irradiation has increased the blocked conductivity for each of the dose rates used in this experiment.

The fact that the blocked conductivity shows a temperature dependence with the activation energy associated with the motion of the anion vacancy and that the magnitude of the blocked conductivity increases with decreasing grain size in polycrystalline specimens seems to imply that the concentration of anion vacancies participating in polarization behavior is extrinsically set, possibly by the concentration of boundaries and other defects such as dislocations in the crystal. The presence of subgrain boundaries may also play a role in this process, and account in part for the presence of the blocked conductivity in annealed single

Figure 11. Blocked conductivity versus reciprocal temperature for unirradiated sodium chloride and for sodium chloride during gamma irradiation at gamma ray dose rates of 2.73×10^3 rad/min, 5.46×10^3 rad/min and 1.09×10^4 rad/min

Key
- – – – unirradiated
- ——— ⊙ 2.73×10^3 rad/min
- — – – — x 5.46×10^3 rad/min
- — – — + 1.09×10^4 rad/min

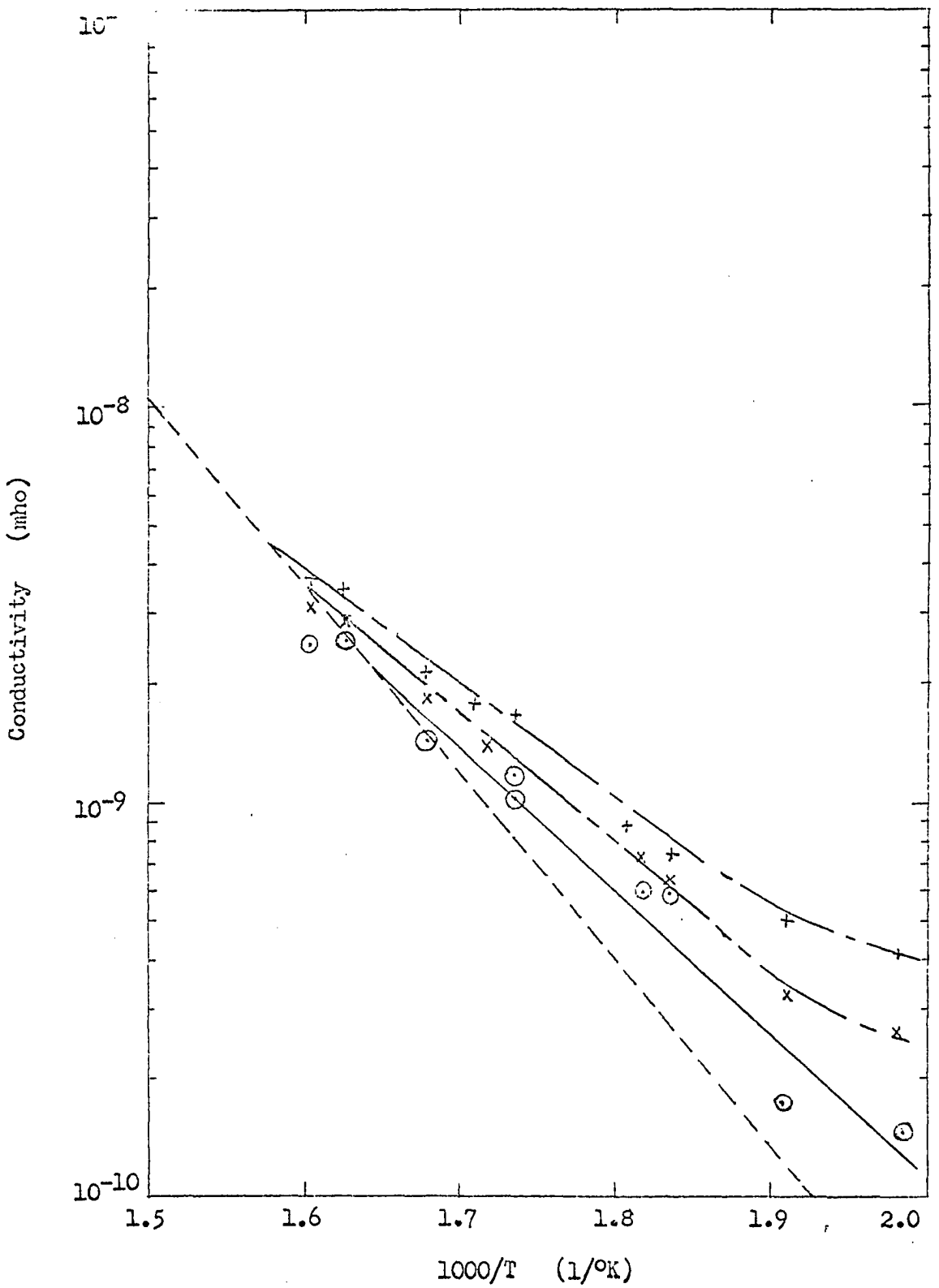
10⁻
10⁻⁸
10⁻⁹
10⁻¹⁰
Conductivity (mho)
1.5
1.6
1.7
1.8
1.9
2.0
1000/T (1/°K)

crystalline material.

If internal subgrain boundaries and defects are assumed to act as sinks for the excess anion vacancies introduced by irradiation (59, 60), and anion vacancies in the volume surrounding these subgrains and defects are assumed to be the source of the blocked conductivity, an increase in blocked conductivity could be due to the increase in anion vacancy concentration as the radiation induced vacancies diffuse to these defects (59, 60). The decrease in activation energy with increasing radiation dose is probably due to the higher concentration of radiation induced anion vacancies existing in the crystal at lower temperatures due to the lower anion vacancy diffusion rate at lower temperatures.

SUMMARY AND CONCLUSIONS

The results of this experiment can be summarized by the following points.

1. The steady state d.c. conductivity for sodium chloride decreases with increasing absorbed dose until a saturation level is reached. The saturation conductivity remains constant for absorbed doses up to 8×10^5 rad, and is lower than the conductivity of the unirradiated material for dose rates of 2.73×10^3, 5.46×10^3 and 1.09×10^4 rad/min.

2. The activation energy for the steady state d.c. conductivity of sodium chloride during Co-60 irradiation at 2.73×10^3 rad/min is higher than for the unirradiated material, but decreases with increasing dose rate.

3. The blocked conductivity of sodium chloride increases during Co-60 irradiation. The increase in blocked conductivity is dose rate dependent, increasing progressively with increasing dose rate.

4. The activation energy for the blocked conductivity decreases progressively with increasing dose rate for dose rates between 2.73×10^3 and 1.09×10^4 rad/min.

If an additional term is added to account for the photo-induced carriers of lower activation energy which are assumed to be produced during irradiation the results for the steady state d.c. conductivity during irradiation are compatible with mechanisms previously proposed on the basis of conductivity measurements taken after removal of the sample from the irradiation field.

The results for the blocked conductivity were compatible with the assumption that the blocked conductivity is due to anion vacancies. The decrease in the activation for the blocked conductivity is compatible with the increasing concentration of irradiation induced anion vacancies found in color center studies as the irradiation temperature is decreased.

SUGGESTIONS FOR FURTHER WORK

A useful experiment might be carried out to evaluate the importance of cation vacancy production during irradiation of alkali halides by irradiating a material such as cesium bromide or cesium iodide in which the charge transport has been found to be ionic conduction by the halide ion vacancy (72). If positive ion vacancies are produced in these materials during irradiation, they should produce an increase in the time dependent conductivity, in the same manner that the excess halide ion vacancies produced additional conduction in sodium chloride.

Another area for examination which might prove helpful in evaluating blocked conductivity behavior would be an experiment in which sodium chloride crystals would be subjected to plastic deformation to evaluate the effect of dislocations if any on blocked conduction in sodium chloride. If dislocations are effective in increasing the magnitude of the blocked conduction, it would also be interesting to observe the effect of irradiation on the blocked conductivity, since the extra dislocations should provide additional sinks for irradiation induced anion vacancies, leading to a lower concentration of the irradiation induced vacancies and less blocked conductivity enhancement as the dislocation content increased.

ACKNOWLEDGMENTS

I would like to thank Dr. Glenn Murphy for making financial assistance available throughout the work leading to the Ph. D., and for his valuable advice throughout the same period.

I would also like to thank Dr. J. C. Picken for his advice during preparation of the irradiation chamber, help in carrying out the irradiations and for doing the dosimetry measurements for this experiment.

Finally, I would like to thank my wife for her help.

BIBLIOGRAPHY

1. Vul, B. M. The effect of gamma radiation on the electrical conductivity of insulators. Sov. Phys.-Sol. St. 3: 1644-1650. 1962.

2. Dau, G. J. and Davis, M. V. Gamma-induced electrical conductivity in alumina. Nuc. Sci. and Eng. 25: 223-226. 1966.

3. Dreyfus, R. W. and Nowick, A. S. Energy and entropy of formation and motion of vacancies in NaCl and KCl crystals. J. of Appl. Phys. 31: 473-477. 1962.

4. Graham, H. C., Tallan, N. M. and Russell, R., Jr. Particle size dependence of the electrical conductivity of NaCl. J. of Am. Cer. Soc. 50: 156-163. 1967.

5. Dreyfus, R. W. and Nowick, A. S. Ionic conductivity of doped NaCl crystals. Phys. Rev. 126: 1367-1377. 1962.

6. Wert, C. A. and Thomson, R. M. Physics of solids. New York, N.Y., McGraw-Hill Book Co., Inc. 1964.

7. Dreyfus, R. W. Dielectric relaxation due to impurity-vacancy complexes in NaCl crystals. Phys. Rev. 121: 1675-1687. 1961.

8. Dreyfus, R. W. and Laibowitz, R. B. Anelastic and dielectric relaxation due to impurity-vacancy complexes in NaCl crystals. Phys. Rev. 135: 1413-1422. 1964.

9. Kliewer, K. L. and Koehler, J. S. Space charge in ionic crystals. Phys. Rev. 140: A1226-A1240. 1965.

10. Barr, L. W., Morrison, J. A. and Schroeder, P. A. Anion diffusion in crystals of NaCl. J. of Appl. Phys. 36: 624-631. 1965.

11. Laurence, N. Self-diffusion of the chloride ion in sodium chloride. Phys. Rev. 120: 57-62. 1960.

12. Laurent, J. R. and Bénard, J. Autodiffusion des ions dans les cristoux uniques des haloginures de potassium et des chlorures alcolins. J. Phys. and Chem. Sol. 3, Nos. 1/2: 7-19. 1957.

13. Fumi, F. G. and Tosi, M. P. Lattice calculations on point imperfections in the alkali halides. Disc. Fara. Soc. 23: 92-98. 1957.

14. Allnatt, A. R. and Jacobs, P. W. M. A. C. polarization effects in the ionic conductivity of potassium chloride crystals. J. Phys. and Chem. Sol. 19, Nos. 3/4: 281-290. 1961.

15. Wimmer, J. M. and Tallan, N. M. Interfacial polarization in single crystal NaCl. J. of Appl. Phys. 37: 3728-3733. 1966.

16. Jacobs, P. W. M. and Maycock, J. N. Polarization effects in the ionic conductivity of alkali halide crystals. I. AC capacity. J. Chem. Phys. 39: 757-762. 1963.

17. Duerig, W. H. and Markham, J. J. Color centers in alkali halides at 5°K. Phys. Rev. 88: 1043-1049. 1952.

18. Rabin, H. and Klick, C. C. Formation of F centers at low and room temperatures. Phys. Rev. 117: 1005-1010. 1960.

19. Gordon, R. B. and Nowick, A. S. Structure sensitivity of the x-ray coloration of NaCl crystals. Phys. Rev. 101: 977-983. 1956.

20. Ritz, V. H. Vacancy-production efficiencies in KBr at low temperatures. Phys. Rev. 142: 505-513. 1966.

21. Bauer, C. L. and Gordon, R. B. Structure sensitivity of F-center generation by x-rays at low temperatures. Phys. Rev. 126: 73-78. 1962.

22. Mitchell, P. V. and Wiegand, D. A. Formation of F-centers in KCl by x-rays. Phys. Rev. 121: 484-498. 1961.

23. Etzel, H. W. Enhancement of the F- and V-bands in sodium chloride containing calcium. Phys. Rev. 87: 906-907. 1952.

24. Ikeya, M., Itoh, N., Okada, T. and Suita T. Study of enhancement x-ray coloration of NaCl by divalent impurities. J. Phys. Soc. Jap. 21: 1304-1309. 1966.

25. Harrison, P. G. Experimental investigation of the effect of irradiation intensity on the productions of F centers in NaCl. J. Chem. Phys. 37: 388-392. 1962.

26. Faraday, B. J. and Compton, W. D. Color centers produced in KCl and KBr by prolonged x-irradiation at low temperatures. Phys. Rev. 138: A893-A911. 1965.

27. Schnatterly, S. and Compton, D. W. F-aggregate color centers in KCl. Phys. Rev. 135: A227-A232. 1964.

28. Pung, L. A. and Khaldre, Y. Y. Temperature stability of self-trapped holes in some alkali metal halide single crystals. Acad. Sci. Bul., Phys. Ser., 30: 1509-1511. 1966.

29. Sonder, E., Sibley, W. A., Rowe, J. E. and Nelson, C. M. Some properties of defects produced by ionizing radiation in KCl between 80°K and 300°K. Phys. Rev. 153: 1000-1008. 1967.

30. Strumen, R., Nihaul, J., Geversand, R. and Amelinckx, A., eds. The interaction of radiation with solids. New York, N.Y., John Wiley and Sons. 1964.

31. Seitz, F. Color centers in alkali halide crystals. Rev. Mod. Phys. 26: 7-94. 1954.

32. Varley, J. H. O. Discussion of some mechanisms of F-centre formation in alkali halides. J. Phys. and Chem. Sol. 23: 985- 1005. 1962.

33. Howard, R. E., Voska, S. and Smoluchowski, R. Mechanism for production of interstitials in KCl by x rays at low temperature. Phys. Rev. 122: 1406-1408. 1961.

34. Klick, C. C. Mechanism for coloration of alkali halides at low temperatures. Phys. Rev. 120: 760-762. 1960.

35. Williams, F. E. Theory of defect formation in alkali halides by ionizing radiation. Phys. Rev. 126: 70-72. 1962.

36. Ritz, V. H. F-center production efficiencies. Phys. Rev. 133: A1452-A1470. 1964.

37. Durap, J. and Platzman, R. L. Role of the auger effect in the displacement of atoms in solids by ionizing radiation. Disc. Fara. Soc. 31: 156. 1961.

38. Crawford, J. H., Jr., Sibley, W. H. and Sonder, E. The influence of electron-trapping impurity in defect creation and bleaching in KCl irradiated at 78°K. Phys. Stat. Sol. 23: 301-306. 1967.

39. Crowe, G. J., Fuchs, W. and Weigand, D. A. Schottky disorder and lattice relaxation in single crystals of NaCl due to x-irradiation at room temperature. Phys. Rev. Let. 16: 1154-1155. 1966.

40. Hersh, H. N. Proposed excitonic mechanism of color-center formation in alkali halides. Phys. Rev. 148: 928-932. 1960.

41. Pooley, D. F centre production in alkali halides by radiationless electron hole recombination. Sol. St. Comm. 3: 241-243. 1965.

42. Luschchik, C. B., Liidya, G. G. and Elango, M. A. Electron-hole mechanism of color center creation in ionic crystals. Sov. Phys.-Sol. St. 6: 1784-1794. 1965.

43. Vilu, R. O. and Elango, M. A. Role of hole processes in the formation of F-centers in ionic crystals during the initial stage of radiation-induced coloration. Sov. Phys.-Sol. St. 7: 2967-2968. 1966.

44. Giuliani, G. and Reguzzoni, E. X-ray production and thermal annealing of Frenkel pairs in KCl. Phys. Stat. Sol. 25: 437-448. 1968.

45. Sonder, E. and Sibley, W. A. Radiation equilibrium of F and M centers in KCl. Phys. Rev. 129: 1578-1582. 1963.

46. Pretzel, F. E. Radiation damage to alkali halides and other simple ionic crystals. U.S. Atomic Energy Commission Report LA-3387 [Los Alamos Scientific Lab., N.Mex.] 1960.

47. Harrison, P. G. Effect of x-ray intensity on the production of color centers in NaCl and KCl. Phys. Rev. 131: 2505-2511. 1963.

48. Nelson, C. M., Sproull, R. L. and Coswell, R. S. Conductivity changes in KCl produced by γ and n irradiation. Phys. Rev. 90: 364. 1953.

49. Billington, D. S. and Crawford, J. H. Radiation damage in solids. Princeton, N.J., Princeton University Press. 1961.

50. Pearlstein, E. Change of electrical conductivity of sodium chloride upon bombardment with high-energy protons. Phys. Rev. 92: 881-882. 1953.

51. Seitz, F. Color centers in alkali halide crystals. Rev. Mod. Phys. 18: 394-408. 1946.

52. Kobayashi, K. Annealing of irradiation effects in sodium chloride irradiated with high-energy protons. Phys. Rev. 102: 348-355. 1956.

53. Krasnopevtseu, V. V. Dielectric properties of KBr single crystals irradiated with fast electrons. Sov. Phys.-Sol. St. 5: 1645-1650. 1964.

54. Ignatéva, M. I., Zavadovskaya, E. K. and Malik-Gaikazyan, I. Y. Effect of divalent impurities on the radiation stability of alkali-halide crystals. Sov. Phys.-Sol. St. 5: 2031-2034. 1964.

55. Pershits, Y. N., Gutman, V. I. and Anosova, A. I. The effect of foreign ions on the electric conductivity of irradiated alkali halide crystals (translated title). Izv. Vysshikh Uchebn. Zavedenci Fiz. 1: 3-7. 1964. Original not available: abstracted in Nuc. Sci. Ab. 18, No. 12: 2780. 1964.

56. Rozman, G. A. Correlation between divalent cation impurity and dipolon concentrations in alkali-halide crystals. Sov. Phys.-Sol. St. 9: 2392-2393. 1968.

57. Hayes, W. and Nichols, G. M. Paramagnetic resonance and optical absorption of a V center. Phys. Rev. 117: 993-998. 1960.

58. Malik-Gaikezyan, I. Y., Zavadovskaya, E. K. and Ignatéva, M. I. Change in the electrical conductivity of KCl crystals with divalent impurity admixtures after irradiation with x-rays. Sov. Phys.-Sol. St. 6: 967-968. 1964.

59. Christy, R. W. and Harte, W. E. Electrical conductivity of x-irradiated NaCl. Phys. Rev. 109: 710-715. 1958.

60. Christy, R. W. and Fukushima, E. Electrical conductivity of x-irradiated KCl. Phys. Rev. 118: 1222-1225. 1960.

61. Ewles, J. and Jain, S. C. Diffusion of negative ion vacancies in potassium chloride. Proc. Roy. Soc. (London) Series A, 243: 353-358. 1958.

62. Éidelman, L. G. Block boundaries in sodium chloride single crystals grown from the melt. Sov. Phys.-Sol. St. 9: 9-14. 1967.

63. Hacke, J. Über die Beeinflussung der Ionenleitfähigkeit von NaCl durch Roentgenstrahlung. Ztschr. Phys. 155: 628-635. 1959.

64. Royce, B. S. H. Effect of ionizing radiation on alkali halides. Am. Soc. for Test. and Mat. Spec. Tech. Pub. 359. 1963.

65. Guccione, R., Tosi, M. P. and Asdente, M. Migration barriers for cations and anions in alkali halide crystals. J. Phys. and Chem. Sol. 10: 162-168. 1959.

66. Tharmalingam, K. Interstitial mobility in NaCl. J. Phys. and Chem. Sol. 24: 1380-1382. 1963.

67. Hatcher, R. D. and Dienes, G. J. Relaxation and activation energies for an interstitial neutral defect in an alkali halide lattice. Phys. Rev. 124: 726-735. 1961.

68. Hayes, W. Effects of ionizing radiations on alkali halides containing divalent impurities. J. of Appl. Phys. 33: 329-331. 1962.

69. Itoh, N., Royce, B. S. H. and Smoluchowski, R. Recombination of vacancies and interstitials in KBr at low temperatures. Phys. Rev. 137: A1010-A1015. 1965.

70. Mapother, D. Effect of x-ray irradiation on the self-diffusion coefficient of Na in NaCl. Phys. Rev. 89: 1231-1232. 1953.

71. Röhrig, H. and Scharmann, A. Über den Einfluss von Röntgenstrahlung auf die Ionenleitfähigkeit von KBr. Ztschr. Phys. 184: 191-197. 1965.

72. Lynch, D. W. Diffusion and ionic conductivity in cesium bromide and cesium iodide. Phys. Rev. 118: 468-473. 1960.

APPENDIX

Steady State d.c. Conductivity Measurements

A modified Wheatstone bridge is shown in Figure 12, where R_1 and

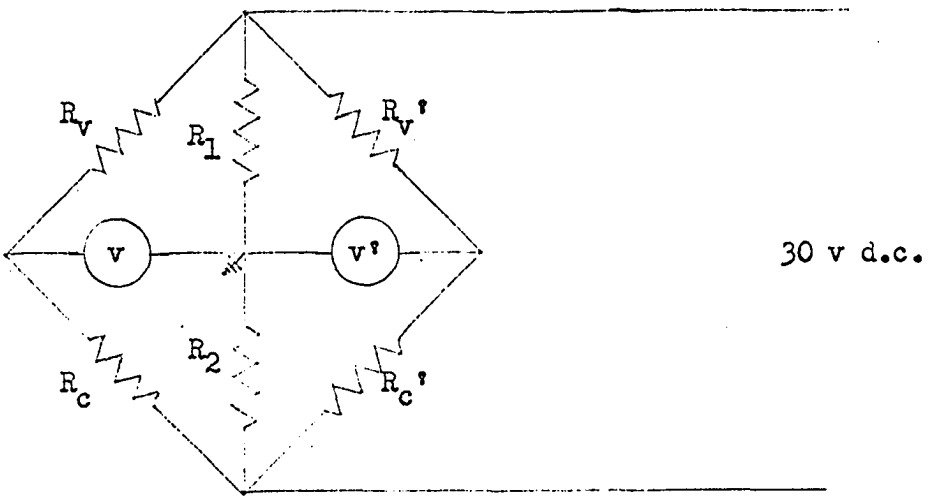

Figure 12. Conductivity bridge used for experiment

R_2 represent resistors which are set up to allow various multipliers of from 1 to 10^6, R_v and R_v' represent continuously variable 50,000 ohm resistances having a linearity of $\pm$ 0.25% and R_c and R_c' represent the crystal resistance in the guarded conductivity circuit and the guard circuit resistance respectively. Hewelett-Packard model vacuum tube voltmeters were used for null measurements. At null, the crystal resistance is given by the expression

$$R_c = \frac{R_v \cdot R_2}{R_1}$$

$$= (5.06 \times 10^{(n+4)} - 5.06 \times 10^{(n+3)} P)$$

for even multipliers and

$$R_c = (5.28 \times 10^{(n+4)} - 5.28 \times 10^{(n+3)} P)$$

for odd multipliers, where P is the dial reading for R_v and n is the multiplier.

The conductivity is related to the crystal resistance by the relationship

$$\sigma = \frac{t}{AR_c}$$

where t is the crystal thickness and A is the conduction area. The crystal used in these measurements was 0.1215 cm thick and the conduction area was 0.327 cm^2.

The conductivity of the crystal was calculated using the relationships

$$\sigma = \frac{1}{1.37 \times 10^{(n+5)} - 1.37 \times 10^{(n+4)} P}$$

for even multipliers and

$$\sigma = \frac{1}{1.42 \times 10^{(n+5)} - 1.42 \times 10^{(n+4)} P}$$

for odd multipliers.

Time-Dependent Conductivity Measurements

Examination of Figure 12 shows that the out of balance voltage, V, appearing when the conductivity of the crystal is increased by polarity reversal is given by the relationship

$$\left(\frac{R_v}{R_v + R_c}\right)30 - \left(\frac{R_1}{R_1 + R_2}\right)30 = V.$$

For all of the irradiation conductivity measurements, the resistance R_2 was greater than R_1 by a factor of at least 1000 and R_c was greater than R_v by a factor of at least 1000. Then

$$R_c = \frac{R_v}{\left(\frac{R_1}{R_2} + \frac{V}{30}\right)}$$

from which the crystal conductivity for the bridge out of balance by V volts can be calculated by the relationship

$$\sigma = \frac{t}{AR_c}$$

$$= \frac{t\left(\frac{R_1}{R_2} + \frac{V}{30}\right)}{AR_v}$$

$$= \sigma_{\text{steady state}} + \left(\frac{V\,R_2}{30\,R_1}\right)\sigma_{\text{steady state}}.$$

Data Tables

Table 1. Conductivity measurements for unirradiated sodium chloride

Run number	Bridge reading units	Bridge multiplier	Δ recorder divisions	Calibration sensitivity mv/div.	Bridge unbalance mv	Unblocked conductivity $ohm^{-1}cm^{-1}$	Blocked conductivity $ohm^{-1}cm^{-1}$	$\frac{1000}{T}$ $1/^{o}K$
1	3.37	10^6	4	0.002	0.008	$1.102X10^{-11}$	$2.94X10^{-12}$	2.251
2	2.90	10^5	15.5	0.002	0.031	$9.94X10^{-11}$	$1.03X10^{-11}$	2.091
3	2.48	10^5	36	0.002	0.072	$2.80X10^{-10}$	$6.72X10^{-11}$	2.015
4	9.00	10^5	11.3	0.002	0.034	$7.09X10^{-10}$	$8.0X10^{-11}$	1.928
5	5.98	10^4	38	0.015	0.57	$1.83X10^{-9}$	$3.48X10^{-10}$	1.805
6	2.26	10^3	19	0.3	2.85	$9.11X10^{-9}$	$1.30X10^{-9}$	1.636
7	1.57	10^3	14	0.3	5.2	$8.35X10^{-9}$	$1.44X10^{-9}$	1.631
8	6.94	10^3	19	0.3	5.7	$2.30X10^{-8}$	$4.37X10^{-9}$	1.529
9	1.23	10^3	39	0.3	11.7	$8.35X10^{-8}$	$3.26X10^{-8}$	1.420
10	6.84	10^2	25	3	75	$2.32X10^{-7}$	$5.81X10^{-8}$	1.355
11	4.47	10^1	84	3	0.252v	$1.35X10^{-6}$	$1.4X10^{-7}$	1.249
12	8.79	10^1	21	30	0.63v	$6.10X10^{-6}$	$0.79X10^{-7}$	1.187
13	9.43	10^6	4	0.002	0.004	$1.27X10^{-10}$	$1.69X10^{-11}$	2.115
14	9.50	10^6	3	0.002	0.003	$1.49X10^{-10}$	$1.49X10^{-11}$	2.104

Table 1 (Continued)

Run number	Bridge reading units	Bridge multiplier	Δ recorder divisions	Calibration sensitivity mv/div.	Bridge unbalance mv	Unblocked conductivity $ohm^{-1}cm^{-1}$	Blocked conductivity $ohm^{-1}cm^{-1}$	$\frac{1000}{T}$ $1/^{o}K$
15	8.53	10^5	16	0.002	0.032	$4.81X10^{-10}$	$5.13X10^{-11}$	1.998
16	8.68	10^5	10	0.002	0.020	$5.35X10^{-10}$	$3.56X10^{-11}$	1.989
17	9.30	10^5	15.5	0.002	0.031	$1.03X10^{-9}$	$1.05X10^{-10}$	1.918
18	9.27	10^5	15	0.002	0.030	$1.01X10^{-9}$	$1.01X10^{-10}$	1.921
19	6.30	10^4	30	0.015	0.45	$2.71X10^{-9}$	$4.06X10^{-10}$	1.815
20	7.99	10^4	12	0.05	0.60	$3.66X10^{-9}$	$7.32X10^{-10}$	1.734
21	8.03	10^4	19.5	0.05	0.975	$3.74X10^{-9}$	$1.21X10^{-9}$	1.734
22	0.42	10^3	62	0.1	6.2	$7.36X10^{-9}$	$1.47X10^{-9}$	1.672
23	0.55	10^3	62	0.1	6.2	$7.46X10^{-9}$	$1.49X10^{-9}$	1.667
24	5.43	10^3	17.5	0.3	5.25	$1.54X10^{-8}$	$2.69X10^{-9}$	1.592
25	5.16	10^3	15	0.3	7.5	$1.46X10^{-8}$	$2.19X10^{-9}$	1.588
26	5.26	10^6	4	0.002	0.008	$1.035X10^{-11}$	$2.94X10^{-12}$	2.282
27	8.71	10^5	14	0.002	0.016	$5.53X10^{-10}$	$5.33X10^{-11}$	2.002
28	8.38	10^3	14.5	0.3	4.35	$4.42X10^{-8}$	$1.92X10^{-8}$	1.482

Table 1 (Continued)

Run number	Bridge reading units	Bridge multiplier	Δ recorder divisions	Calibration sensitivity mv/div.	Bridge unbalance mv	Unblocked conductivity $ohm^{-1}cm^{-1}$	Blocked conductivity $ohm^{-1}cm^{-1}$	$\frac{1000}{T}$ $1/°K$
29	7.85	10^2	91	3	0.273v	$3.41X10^{-7}$	$1.03X10^{-7}$	1.322
30	1.03	10^1	18	30	0.54v	$8.22X10^{-7}$	$1.9X10^{-7}$	1.278
31	7.09	10^1	14	30	0.42v	$2.54X10^{-6}$	$4.6X10^{-7}$	1.204

Table 2. Unblocked conductivity measurements during gamma ray irradiation of sodium chloride

Run number	Temperature ^{o}K	$\frac{1000}{T}$ $1/^{o}K$	Bridge reading units	Bridge multiplier	Unblocked conductivity $ohm^{-1}cm^{-1}$	Dose rate rad/min
1	323	1.679	8.94	10^4	$6.68X10^{-9}$	$2.73X10^3$
1	323	1.679	8.93	10^4	$6.57X10^{-9}$	$5.46X10^3$
1	323	1.679	8.92	10^4	$6.48X10^{-9}$	$10.9X10^3$
2	251	1.908	8.70	10^5	$5.43X10^{-10}$	$2.73X10^3$
2	251	1.908	8.89	10^5	$6.28X10^{-10}$	$5.46X10^3$
2	251	1.908	9.06	10^5	$7.39X10^{-10}$	$10.9X10^3$
3	278	1.816	6.47	10^4	$1.66X10^{-9}$	$2.73X10^3$
3	278	1.816	6.56	10^4	$1.70X10^{-9}$	$5.46X10^3$
3	280	1.808	6.80	10^4	$1.83X10^{-9}$	$10.9X10^3$
4	351	1.602	4.58	10^3	$1.30X10^{-8}$	$2.73X10^3$
4	351	1.602	4.37	10^3	$1.25X10^{-8}$	$5.46X10^3$
4	351	1.602	4.13	10^3	$1.20X10^{-8}$	$10.9X10^3$
5	304	1.735	7.84	10^4	$3.78X10^{-9}$	$2.73X10^3$
5	308	1.719	8.07	10^4	$4.43X10^{-9}$	$5.46X10^3$

Table 2 (Continued)

Run number	Temperature °K	1000/T 1/°K	Bridge reading units	Bridge multiplier	Unblocked conductivity $ohm^{-1}cm^{-1}$	Dose rate rad/min
5	313	1.708	8.47	10^4	$4.82X10^{-9}$	$10.9X10^3$
6	273	1.834	4.23	10^4	$1.27X10^{-9}$	$2.73X10^3$
6	274	1.830	4.51	10^4	$1.33X10^{-9}$	$5.46X10^3$
6	274	1.830	5.14	10^4	$1.51X10^{-9}$	$10.9X10^3$
7	304	1.735	7.72	10^4	$3.23X10^{-9}$	$2.73X10^3$
7	304	1.735	7.99	10^4	$3.65X10^{-9}$	$10.9X10^3$
8	342	1.626	3.50	10^3	$1.09X10^{-8}$	$2.73X10^3$
8	342	1.626	3.02	10^3	$1.05X10^{-8}$	$5.46X10^3$
8	343	1.622	2.83	10^3	$9.84X10^{-9}$	$10.9X10^3$
9	232	1.981	7.37	10^5	$2.68X10^{-10}$	$2.73X10^3$
9	234	1.981	7.60	10^5	$2.94X10^{-10}$	$5.46X10^3$
9	234	1.974	7.94	10^5	$3.44X10^{-10}$	$10.9X10^3$

Table 3. Blocked conductivity measurements during gamma ray irradiation of sodium chloride

Run number	Bridge reading units	Bridge multiplier	Δ recorder divisions	Calibration sensitivity mv/div.	Bridge unbalance mv	$\frac{1000}{T}$ 1/°K	Blocked conductivity $ohm^{-1}cm^{-1}$	Dose rate rad/min
1	8.94	10^4	58	0.1	5.8	1.679	$1.29X10^{-9}$	$2.73X10^3$
1	8.93	10^4	83	0.1	8.3	1.679	$1.83X10^{-9}$	$5.46X10^3$
1	8.92	10^4	98	0.1	9.75	1.679	$2.11X10^{-9}$	$10.9X10^3$
2	8.70	10^5	46	0.002	0.092	1.908	$1.69X10^{-10}$	$2.73X10^3$
2	8.89	10^5	79	0.002	0.158	1.908	$3.28X10^{-10}$	$5.46X10^3$
2	9.06	10^5	100	0.002	0.20	1.908	$4.95X10^{-10}$	$10.9X10^3$
3	6.47	10^4	71	0.015	1.07	1.816	$5.93X10^{-9}$	$2.73X10^3$
3	6.56	10^4	83	0.015	1.25	1.816	$7.10X10^{-9}$	$5.46X10^3$
3	6.80	10^4	28	0.05	1.40	1.808	$8.47X10^{-9}$	$10.9X10^3$
4	4.58	10^3	19	0.3	5.7	1.602	$2.52X10^{-9}$	$2.73X10^3$
4	4.37	10^3	25	0.3	7.5	1.602	$3.11X10^{-9}$	$5.46X10^3$
4	4.13	10^3	30	0.3	9.0	1.602	$3.64X10^{-9}$	$10.9X10^3$
5	7.84	10^4	8.7	0.1	0.87	1.735	$1.17X10^{-9}$	$2.73X10^3$
5	8.07	10^4	9.4	0.1	0.94	1.719	$1.39X10^{-9}$	$5.46X10^3$
5	8.19	10^4	11	0.1	1.08	1.708	$1.72X10^{-9}$	$10.9X10^3$

Table 3 (Continued)

Run number	Bridge reading units	Bridge multiplier	Δ recorder divisions	Calibration sensitivity mv/div.	Bridge unbalance mv	$\frac{1000}{T}$ 1/°K	Blocked conductivity $ohm^{-1}cm^{-1}$	Dose rate rad/min
6	4.23	10^4	47	0.3	1.41	1.834	$5.93X10^{-10}$	$2.73X10^3$
6	4.51	10^4	48	0.3	1.44	1.830	$6.34X10^{-10}$	$5.46X10^3$
6	5.14	10^4	48	0.3	1.44	1.830	$7.32X10^{-10}$	$10.9X10^3$
7	7.72	10^4	20	0.05	1.0	1.735	$1.10X10^{-9}$	$2.73X10^3$
7	8.29	10^4	23	0.05	1.15	1.735	$1.68X10^{-9}$	$10.9X10^3$
8	3.50	10^3	24	0.3	7.2	1.626	$2.58X10^{-9}$	$2.73X10^3$
8	3.02	10^3	27	0.3	8.1	1.622	$2.82X10^{-9}$	$5.46X10^3$
8	2.83	10^3	34	0.3	10.2	1.622	$3.41X10^{-9}$	$10.9X10^3$
9	7.37	10^5	8	0.002	0.016	1.981	$1.43X10^{-10}$	$2.73X10^3$
9	7.60	10^5	15	0.002	0.030	1.981	$2.61X10^{-10}$	$5.46X10^3$
9	7.94	10^5	21	0.002	0.042	1.974	$4.12X10^{-10}$	$10.9X10^3$

Error Analysis

The uncertainty in the measured value of the conductivity due to the measuring apparatus and the standard deviation for straight line least square fitting of the measured conductivities of the unirradiated material are shown in Table 4. It appears that the major source of

Table 4. Error analysis results

Variable	Uncertainty due to equipment	Temperature	Deviation of conductivity
Steady state d.c. conductivity	0.3%	225°C	8.9%
Blocked conductivity	0.6%	225°C	16.5%

variation in the measured results for the steady state d.c. conductivity may be the variation of the defect structure in the crystal between runs rather than uncertainty in the conductivity measurements. Extrapolation errors and defect structure changes appear likely to be the major sources of variation for the blocked conductivity values.

The equipment uncertainty was determined by evaluating the uncertainty in each of the components and calculating the total uncertainty in the usual manner.

69-4221

CARLSON, Michael Claudewell Jon, 1939-

THE EFFECT OF GAMMA RADIATION ON THE CONDUCTIVITY OF SODIUM CHLORIDE.

Iowa State University, Ph.D., 1968
Engineering, nuclear

University Microfilms, Inc., Ann Arbor, Michigan